VILNIUS UNIVERSITY
INSTITUTE OF PHYSICS

Jonas Pocius

The dynamics and optimization of the radiation of a femtosecond diode pumped Yb:KGW laser

Summary of doctoral thesis
Physical science, Physics (02 P)

Vilnius, 2009

Doctoral dissertation prepared 2004-2009 at the Vilnius University.

Scientific supervisor:

prof. habil. dr. Algis Petras Piskarskas (Vilnius University, Physical sciences, Physics – 02 P).

Scientific advisor:

dr. Romualdas Danielius (Šviesos konversija Ltd, Physical sciences, Physics 02 P).

Doctoral Dissertation will be defended in the Council of Physics of Vilnius University:

Chairman:

prof. habil. dr. Valdas Sirutkaitis (Vilnius University, Physical sciences, Physics – 02 P).

Members:

prof. dr. Audrius Dubietis (Vilnius University, Physical sciences, Physics – 02 P).

prof. habil. dr. Algirdas Petras Stabinis (Vilnius University, Physical sciences, Physics – 02 P).

prof. habil. dr. Gintautas Jurgis Babonas (Semiconductor Physics Institute, Physical sciences, Physics – 02 P).

dr. Edmundas Širmulis (Semiconductor Physics Institute, Physical sciences, Physics – 02 P).

Oponents:

prof. habil. dr. Gintaras Valušis (Semiconductor Physics Institute, Physical sciences, Physics – 02 P).

dr. Arūnas Varanavičius (Vilnius University, Physical sciences, Physics – 02 P).

The official defence of the Dissertation will be held at 3 p.m. on 21 December 2009 in 510th auditorium at Physics Department of Vilnius University, Saulėtekio ave. 9, bldg. 3, LT-10222 Vilnius, Lithuania.

Summary of the Doctoral Dissertation has been distributed on 20 November 2009.

The Dissertation is available at the libraries of Vilnius University and Institure of Physics.

VILNIAUS UNIVERSITETAS
FIZIKOS INSTITUTAS

Jonas Pocius

Puslaidininkiniais lazeriais kaupinamo Yb:KGW femtosekundinio lazerio veikos dinamika ir spinduliuotės parametrų optimizavimas

Daktaro disertacija
Fiziniai mokslai, fizika (02 P)

Vilnius, 2009

Disertacija rengta 2004-2009 metais Vilniaus universitete.

Mokslinis vadovas:

prof. habil. dr. Algis Petras Piskarskas (Vilniaus universitetas, fiziniai mokslai, fizika– 02 P).

Konsultantas:

dr. Romualdas Danielius (UAB MGF „Šviesos konversija“, fiziniai mokslai, fizika– 02 P).

Disertacija ginama Vilniaus universiteto Fizikos mokslo krypties taryboje:

Pirmininkas:

prof. habil. dr. Valdas Sirutkaitis (Vilniaus universitetas, fiziniai mokslai, fizika– 02 P).

Nariai:

prof. dr. Audrius Dubietis (Vilniaus universitetas, fiziniai mokslai, fizika– 02 P).

prof. habil. dr. Algirdas Petras Stabinis (Vilniaus universitetas, fiziniai mokslai, fizika– 02 P).

prof. habil. dr. Gintautas Jurgis Babonas (Puslaidininkių fizikos institutas, fiziniai mokslai, fizika– 02 P).

dr. Edmundas Širmulis (Puslaidininkių fizikos institutas, fiziniai mokslai, fizika– 02 P).

Oponentai:

prof. habil. dr. Gintaras Valušis (Puslaidininkių fizikos institutas, fiziniai mokslai, fizika– 02 P).

dr. Arūnas Varanavičius (Vilniaus universitetas, fiziniai mokslai, fizika– 02 P).

Disertacija bus ginama viešame Fizikos mokslo krypties tarybos posėdyje 2009 m. gruodžio mėn. 21 d. 15 val. Vilniaus universiteto Fizikos fakulteto 510-oje auditorijoje. Adresas: Saulėtekio al. 9, 3 korp. LT-10222, Vilnius, Lietuva.

Disertacijos santrauka išsiuntinėta 2009 m. lapkričio mėn. 20 d.

Disertacija galima peržiūrėti Vilniaus universiteto ir Fizikos instituto bibliotekose.

Table of Contents

Introduction

After the demonstration of the first laser in 1960 it was stated that there was a solution looking for a problem [1]. After some time a number of possible applications were suggested like spectroscopy, distance measurements and pollution detection, fusion, microscopy and communication but one of the most important and more common applications for lasers is material processing.

The interaction of light and matter depends on a light wavelength as well as properties of the matter. Each laser medium has its own emission spectrum determined by its structure of energy levels. The possibility to generate different wavelengths stimulated the search for new laser materials. In 1960 the first gas laser was invented [2], in 1962 the first semiconductor laser followed [3] while in 1966 the first liquid dye laser was demonstrated [4]. The main ideas about another way to generate new wavelengths were published in 1962, they deal with parametric interaction [5, 6]. The way how light will interact with matter depends on light intensity too. In common case the maximum light intensity, $I = \frac{E}{\Delta\tau S}$, depends on pulse energy - E, the pulse duration - $\Delta\tau$ and the minimum beam spot area - S. The minimum beam spot area depends on a radiance wavelength and beam quality and the beam can't be focused onto a smaller spot than its radiance wavelength. Thus to maximize light intensity with a limited beam spot size the pulse energy should be maximized and the pulse duration should be minimized.

Especially high intensities (10^{18} W/cm^2 – 10^{19} W/cm^2) radiance is used for electron beam generation and acceleration [7-10], neutron generation [11, 12] and fusion [13]. 10^8 W/cm^2 – 10^{12} W/cm^2 radiance intensity is used in nonlinear optics application. Radiance higher than ~10^{12} W/cm^2 intensity may ionize solid state matter and produce optical damage [14]. Optical damage threshold for absorbing matter at lower intensities depends on pulse duration and energy density. The lower pulse duration the lower energy density is needed to induce optical damage of the matter [15]. Such correlation is because of the shorter heat diffusion length and smaller heated matter volume for a shorter pulse. The length of heat diffusion $l_{dif} = \sqrt{\tau_{imp}\kappa}$, where τ_{imp} is a pulse duration and κ - heat conductance. For example, in copper this length is $\sim 3\mu m$ for a pulse of 10ns duration. That explains why shorter pulses mean more precise material processing and it

allows getting higher resolution. As it is well known light can't be focused onto a smaller spot than its wavelength is and there comes another key potentiality of ultra short pulses. It is possible to set such energy of an ultra short pulse whose intensity is higher than optical damage threshold only in the center area of the beam. In this way it is possible to process formations smaller than beam spot size [16-18] and much smaller ones are processed by using multi photon polymerization technique [19]. Pulse energies for material processing are in order of a few hundred nanojoules to one milijoule [18, 20-24]. Systems that generate pulses of such energy and duration usually consist of a mode locked oscillator and a regenerative amplifier. The fabrication speed depends on the average output power and the pulse repetition rate which is limited by the speed of the cavity quality modulator inside the regenerative amplifier. The average output power in the solid state laser is limited by thermo-optical effects and mechanical damage caused by stress induced by gradient of the temperature in the laser medium [25]. New types of active medium geometry have been developed to avoid and reduce thermo-optical effects. They are fiber and thin disk technologies but both of them have limited possibilities of being used in femtosecond lasers.

Organic dyes have a very broad emission spectrum, however, and they were widely used for first femtosecond lasers. However, because of their photochemical instability dyes were abandoned after the discovery of solid state materials with a sufficient broad emission spectrum for femtosecond pulse generation. The most widely used solid state material for femtosecond lasers is sapphire doped by titanium ions. Second harmonic of solid state neodymium lasers is the most common pump source for Ti:sapphire lasers, however they are much more complex, expensive and much less reliable and efficient in comparison with diode lasers. Many efforts were devoted to explore new solid state materials for femtosecond lasers after the development of commercially available high average power diode lasers. Chromium, neodymium and particularly ytterbium doped materials showed the best results [26]. The first Yb:YAG laser operating in room temperature was demonstrated in 1991 [27], while the first commercially available directly diode pumped femtosecond laser systems which generate more than $100\mu J$ pulses at kilohertz repetition rates appear in 2003-2004 [28]. These achievements and promising possibilities were the key incentive for Light

Conversion Ltd to initiate the development of directly diode pumped Yb:KGW femtosecond laser for micromachining and pumping of optical parametrical amplifiers. This PhD thesis has been written in line with this initiative.

The main objective of the present work is to investigate the dynamics and to optimize the properties of radiation of the diode pumped Yb:KGW femtosecond MOPA (master oscillator power amplifier) laser system.

Main tasks

1. To perform analysis of various Yb doper laser materials according to specific parameters such as emission bandwidth, fluorescence time, thermal conductivity, absorption and emission cross section and quantum defect.
2. Cavity modeling: the optimization of the length and doping concentration of the active medium, the optimization of the cavity for maximum resistance to thermo-lens effect and the optimization of the cavity for Kerr lens mode locking.
3. The investigation of the dynamics of the Yb:KGW regenerative amplifier;
4. The optimization of the amplified pulse compression.
5. The investigation of the suitability and properties of the complete MOPA Yb:KGW system for the OPA pumping.

Positions to defend

- Yb:KGW is the most optimal laser medium for diode pumped high average power $(\leq 10\ \mathrm{W})$ femtosecond lasers $(\geq 150\ \mathrm{fs})$.
- Tilted pulse amplification is the alternative to chirped pulse amplification method maintaining the rational dimensions of the stretcher and the compressor irrespective of a pulse bandwidth.
- The information about time dependence of the pulse spectral components is obtained by spectral components spreading in a single shot autocorrelator with an angular dispersion optical device. This method enables the unambiguous and simpler characterization of the femtosecond pulse compression in comparison with well known FROG, GRENOUILLI and SPIDER methods.

- The 6 W average power femtosecond laser system capable of generating 200 fs pulses at up to 350 kHz pulse repetition rate or up to 1 mJ energy per pulse has been developed applying the results of the research on the dynamics of diode pumped Yb:KGW oscillator and regenerative amplifier.

Publications

1. Giniūnas L., Pocius J., Danielius R., ***Energy extraction improvement in picosecond amplifiers by pulse tilting*** // Opt. Lett. 2006, No. 31, p. 643-645
2. Molis G., Adomavičius R., Krotkus A., Bertulis K., Giniūnas L., Pocius J., Danielius R., ***Terahertz time-domain spectroscopy system based on femtosecond Yb:KGW laser*** // Electronics Letters 2007, Vol. 43, No.3. p. 190-191.
3. O. D. Mücke, D. Sidorov, P. Dombi, A. Pugžlys, S. Ališauskas, N. Forget, J. Pocius, L. Giniūnas, R. Danielius, and A. Baltuška, ***Multimillijoule Optically Synchronized and Carrier-Envelope-Phase-Stable Chirped Parametric Amplification at 1.5 μm***, in *Ultrafast Phenomena XVI*, edited by P. Corkum, K. Nelson, E. Riedle, R. Schoenlein, and S. De Silvestri (Springer, Berlin, 2008).
4. O. D. Mücke, S. Ališauskas, A. J. Verhoef, A. Pugžlys, A. Baltuška, V. Smilgevičius, J. Pocius, L. Giniūnas, R. Danielius, and N. Forget, ***Self-compression of millijoule 1.5 μm pulses***, Opt. Lett. **34**, 2498 (2009).
5. O. D. Mücke, D. Sidorov, P. Dombi, A. Pugžlys, A. Baltuška, S. Ališauskas, V. Smilgevičius, J. Pocius, L. Giniūnas, R. Danielius, and N. Forget, ***Scalable Yb-MOPA-driven carrier-envelope phase-stable few-cycle parametric amplifier at 1.5 μm***, Opt. Lett. **34**, 118 (2009).

Conference presentations

1. Giniūnas L., Pocius J., Danielius R., Michailovas A., Energy extraction improvement in picosecond amplifiers by pulse tilting // XVI Lietuvos ir Baltarusijos seminaras “Lazeriai ir optinis netiesiškumas”, 2004 m. spalio 27-29 d., Vilnius.
2. Pocius J., Giniūnas L., Danielius R., Stretching and amplification of picosecond pulses in Nd:YAG by tilted pulse technique // Internatiol workshop, Parametric processes and periodical structures / 26-29 September, 2004, Vilnius, Lithuania, p. 86-87.
3. Giniūnas L., Zaukevičius A., Pocius J., Danielius R., Energy extration improvement in picosecond amplifiers by pulse tilting // EPS-QEOD Europhoton Conference / Solid – State and Fiber Coherent Light Sources / Swiss Federal institute of Technology, Lausanne, Switzerland, 29 August – 3 September 2004.
4. Račiukaitis G., Grishin M., Danielius R., Pocius J., Giniūnas L., High repetition rate ps- and fs- lasers for micromachining // ICA/LEO 2006, M1001, Oct. 29-Nov.2, 2006, Phoenix, AZ, USA.

5. Molis G., Adomavičius R., Krotkus A., Bertulis K., Giniūnas L., Pocius J., Danielius R., Terahercų spektroskopinė sistema Yb:KGW lazerio pagrindu // 37-oji Lietuvos Nacionalinė Fizikos konferencija 2007, birželio 11-13 d., Vilnius, S4-52, p.275.
6. Danielius R., Giniūnas L., Pocius J., Didelės galios ir didelio pasikartojimo dažnio Yb femtosekundinė sistema // 37-oji Lietuvos Nacionalinė Fizikos konferencija 2007, birželio 11-13 d., Vilnius, S4-5, p. 228.
7. O. D. Mücke, S. Ališauskas, A. J. Verhoef, A. Pugžlys, V. Smilgevičius, J. Pocius, L. Giniūnas, R. Danielius, and A. Baltuška, ***Efficient 4-Fold Self-Compression of 1.5-mJ Infrared Pulses to 19.8 fs***, talk, *Conference on Ultrafast and Nonlinear Optics UFNO'2009*, Burgas, Bulgaria, September 14-18, 2009.
8. O. D. Mücke, S. Ališauskas, A. J. Verhoef, A. Pugžlys, A. Baltuška, V. Smilgevičius, J. Pocius, L. Giniūnas, and R. Danielius, ***Self-compression of millijoule pulses from a 1.5 μm OPCPA***, invited talk, *UltraFast Optics and High Field Short Wavelength (UFO-HFSW 2009)*, Arcachon, France, August 31-September 4, 2009
9. S. Ališauskas, V. Smilgevičius, A. Piskarskas, O. D. Mücke, A. J. Verhoef, A. Pugžlys, A. Baltuška, J. Pocius, L. Giniūnas, R. Danielius, and N. Forget, ***Self-compression of 1.5 μm CEP stable OPCPA pulses in noble gases to sub-20 fs***, poster P1-10, *Northern Optics 2009*, Vilnius, Lithuania, August 26-28, 2009.
10. S. Ališauskas, V. Smilgevičius, A. Piskarskas, O. D. Mücke, A. J. Verhoef, A. Pugžlys, A. Baltuška, J. Pocius, L. Giniūnas, R. Danielius, and N. Forget, ***12.5-mJ CEP-stable OPCPA at 1.5 μm***, invited talk 1, *Northern Optics 2009*, Vilnius, Lithuania, August 26-28, 2009.
11. O. D. Mücke, A. J. Verhoef, A. Pugžlys, A. Baltuška, S. Ališauskas, V. Smilgevičius, J. Pocius, L. Giniūnas, R. Danielius, and N. Forget, ***Toward Terawatt-Peak-Power Single-Cycle Infrared Fields***, talk NFA3, *Nonlinear Optics 2009*, Honolulu, Hawaii, July 12-17, 2009.
12. O. D. Mücke, A. J. Verhoef, A. Pugžlys, A. Baltuška, S. Ališauskas, V. Smilgevičius, J. Pocius, L. Giniūnas, R. Danielius, and N. Forget, ***Multi-mJ Single-Filament Supercontinuum Generation from IR OPCPA***, talk CF5.3, *CLEO Europe*, Munich, Germany, June 14-19, 2009.
13. O. D. Mücke, A. J. Verhoef, A. Fernandez, L. Zhu, A. Pugžlys, A. Baltuška, S. Ališauskas, V. Smilgevičius, J. Pocius, L. Giniūnas, R. Danielius, C.-H. Liu, K.-H. Liao, and A. Galvanauskas, ***12-mJ IR OPCPA Based on Picosecond Nd Pump and Femtosecond Yb Seed Technologies***, invited talk Th3, *Middle Infrared Coherent Sources (MICS'2009)*, Trouville France, June 8-12, 2009.
14. O. D. Mücke, A. J. Verhoef, A. Pugžlys, A. Baltuška, S. Ališauskas, V. Smilgevičius, J. Pocius, L. Giniūnas, R. Danielius, and N. Forget, ***Infrared Multimillijoule Single-Filament Supercontinuum Generation***, talk JWD6, *CLEO*, Baltimore, Maryland, May 31-June 5, 2009.
15. O. D. Mücke, A. J. Verhoef, A. Pugžlys, A. Baltuška, S. Ališauskas, V. Smilgevičius, J. Pocius, L. Giniūnas, R. Danielius, and N. Forget, ***10-mJ Infrared Phase-Stable Parametric Amplification Based on a Femtosecond Yb-MOPA***, talk WD5, *Advanced Solid-State Photonics*, Denver, CO, February 1-4, 2009.
16. O. D. Mücke, A. Pugžlys, P. Dombi, S. Ališauskas, V. Smilgevičius, N. Forget, J. Pocius, L. Giniūnas, R. Danielius, and A. Baltuška, ***10-mJ Few-Cycle OPCPA at***

1.5 μm, invited talk D2-3-03, *IEEE PhotonicsGlobal@Singapore 2008*, SMU Conference Centre, Singapore, December 8-11, 2008.

17. O. D. Mücke, A. Pugžlys, P. Dombi, A. Baltuška, S. Ališauskas, N. Forget, J. Pocius, L. Giniūnas, and R. Danielius, ***10-mJ Few-Cycle Chirped Pulse Parametric Amplification at 1.5 μm***, invited talk WR1, *21st IEEE/LEOS Annual Meeting*, Newport Beach, CA, November 9-13, 2008.
18. O. D. Mücke, D. Sidorov, P. Dombi, A. Pugžlys, S. Ališauskas, N. Forget, J. Pocius, L. Giniūnas, R. Danielius, and A. Baltuška, ***10-mJ Optically Synchronized CEP-Stable Chirped Parametric Amplifier at 1.5 μm***, invited talk Sa20B(E)-1, *XII International Conference on Quantum Optics and Quantum Information (ICQO 2008)*, Vilnius, Lithuania, September 20-23, 2008.
19. O. D. Mücke, D. Sidorov, P. Dombi, A. Pugžlys, A. Baltuška, S. Ališauskas, J. Pocius, L. Giniūnas, and R. Danielius, ***Multimillijoule Optically Synchronized and Carrier-Envelope-Phase-Stable Chirped Parametric Amplification at 1.5 μm***, talk WED4a.4, *16th International Conference on Ultrafast Phenomena*, Stresa (Lago Maggiore), Italy, June 9-13, 2008.
20. O. D. Mücke, D. Sidorov, P. Dombi, A. Pugžlys, A. Baltuška, S. Ališauskas, J. Pocius, L. Giniūnas, and R. Danielis, ***Multimillijoule Optically Synchronized and CEP-Stabilized Chirped Parametric Amplification at 1.5 μm***, talk CTuEE5, *CLEO*, San Jose, California, May 4-9, 2008.
21. O. D. Mücke, D. Sidorov, P. Dombi, A. Pugžlys, A. Baltuška, S. Ališauskas, J. Pocius, L. Giniūnas, and R. Danielis, ***Multimillijoule Optically Synchronized and Carrier-Envelope-Phase-Stable Chirped Parametric Amplification at 1.5 μm***, postdeadline talk MG1, *Advanced Solid-State Photonics*, Nara-Ken New Public Hall, Nara, Japan, January 27-30, 2008.
22. S. Ališauskas, V. Smilgevičius, A. P. Piskarskas, O. D. Mücke, A. J. Verhoef, A. Pugžlys, A. Baltuška, J. Pocius, L. Giniūnas, R. Danielius, and N. Forget, ***12,5 mJ faziškai moduliuotų impulsų su stabilia nešančiojo dažnio faze parametrinis šviesos stiprinimas 1,5 μm srityje*** (12.5-mJ carrier-envelope phase-stable OPCPA at 1.5 μm), talk 2-5, *38th Lithuanian National Physics Conference (LNFK38)*, Vilnius, Lithuania, June 8-10, 2009.
23. S. Ališauskas, V. Smilgevičius, A. P. Piskarskas, O. D. Mücke, A. J. Verhoef, A. Pugžlys, A. Baltuška, J. Pocius, L. Giniūnas, R. Danielius, and N. Forget, ***Milidžiaulinės energijos kelių optinių ciklų trukmės superkontinuumo generacija ties 1,5 μm*** (Multi-mJ few-optical-cycle supercontinuum generation at 1.5 μm), poster S4-34, *38th Lithuanian National Physics Conference (LNFK38)*, Vilnius, Lithuania, June 8-10, 2009.
24. S. Ališauskas, V. Smilgevičius, A. P. Piskarskas, O. D. Mücke, A. J. Verhoef, A. Pugžlys, A. Baltuška, J. Pocius, L. Giniūnas, R. Danielius, and N. Forget, ***Derinamas stabilios fazės kelių optinių ciklų trukmės parametrinis šviesos stiprintuvas ties 1,5 μm*** (Scalable carrier-envelope phase-stable few-optical-cycle parametric amplifier at 1.5 μm), poster S4-33, *38th Lithuanian National Physics Conference (LNFK38)*, Vilnius, Lithuania, June 8-10, 2009.

1. Diode pumped solid state femtosecond lasers

Laser diodes in comparison with flash lamps are much more effective sources for pumping of solid state lasers because of a number of their advantages. First of all, they have a narrower emission spectrum in comparison with lamp sources, which enables good overlap between active medium absorption and laser emission spectrum, and in addition, it is possible to tune the central wavelength of the diode laser by changing its temperature. The characteristic $d\lambda/dT$ value is about 0.3 nm/K. All this enables to use higher pump intensities without worrying about thermo-optical phenomenon. Secondly, the lifetime and the reliability of the whole system are longer because of about 10 times longer lifetime of a diode laser. Thirdly, the laser diodes emit polarized light and it is possible to reshape their beam in order to make the same beam quality in traverse directions. The beam quality is expressed by M^2 value which shows how much the parameters of the generated beam differ from those of the ideal Gaussian beam. The better beam quality allows focusing the beam onto smaller spot size and the waist length is longer. This enables to overlap pump beam with generation beam spatially. Fourthly, a small size of such pump source allows creating small and universal laser systems such as end-pumped solid-state lasers, fiber laser and others. Besides, there is no need of high voltage supply units used by flash lamps. Only 2-3% of pump power is converted into laser radiation and the highest efficiency of 6.3% is reached [29-31] by flash lamp pumped lasers, whereas 65% of optical efficiency is reached by the diode pumped Yb:YAB laser at room temperature and 74% of optical efficiency is demonstrated by the diode pumped Yb:YAG laser at 70K.

InGaAs semiconductor lasers provide the suitable wavelength to pump ytterbium doped laser medium [32]. Nowadays commercially available diode lasers with a 100 μm emitting aperture provide up to 5 W average power, whereas 10 mm width laser diode bars emit up to 60 W. More powerful pump sources may be created by combining a number of laser diode bars.

Pumping schemes for the bulk laser medium

End-pumped and side-pumped schemes are the most common for the bulk laser medium (see Fig. 1). The higher optical to optical efficiency is reached in end-pumped lasers, furthermore, the good matching of spatial pump and generation beams allows generating TEM_{00} mode easier. However, the thermo-optical phenomenon appears in the end pumped laser medium because of some intensity distribution of pump beam and it is the limiting factor of maximum output power. The thermo-optical phenomenon is weaker in the side pumped bulk laser medium because the entire medium is pumped homogeneously however, in this case spatial modes of higher order are amplified as well. The end pumped laser scheme is more favorable for applications where good beam quality is needed more than maximum output power, because reabsorption in the non-pumped medium area acts like soft aperture for higher order spatial modes.

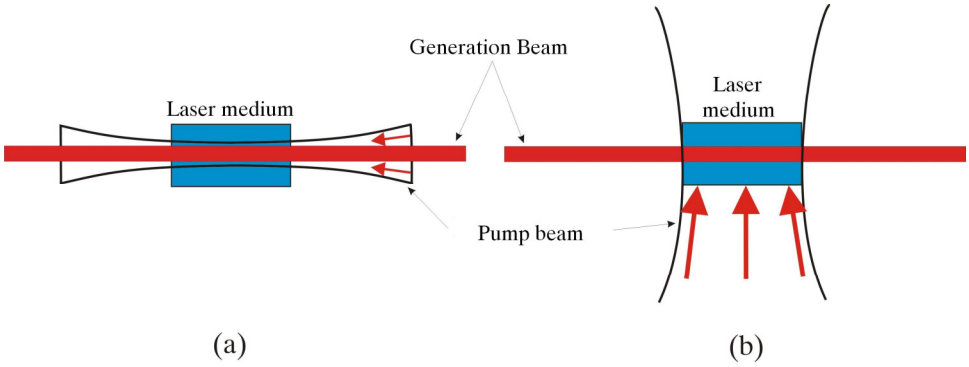

Fig.1. Pumping schemes for bulk laser medium

Diode pumped chromium, neodymium and ytterbium doped lasers

The development of high average power laser diodes generating at 600-1000nm wavelengths enables the direct pumping of chromium, neodymium and ytterbium doped lasers and stimulates the research of new materials for high average power femtosecond lasers. 67 fs pulses were generated by Cr:LiSGAF Kerr lens mode-locked laser, although the pulse energy of only 1 μJ is reached after the amplification with a Cr:LiSGAF regenerative amplifier [33]. 12 fs pulses were generated by Kerr lens mode-locked Cr:LiSAF and Cr:LiCAF oscillators [34, 35]. 90 fs pulses were generated at 235 MHz repetition rate with a new cavity design laser where laser crystal is placed between the pair prisms for dispersion compensation [36]. 20 fs pulses at 400 mW

average power were generated with a Cr^{4+}:YAG laser with chirped mirrors for dispersion compensation. The pulse energy of 10.5 μJ was measured after the amplification with a Cr:LiSGAF regenerative amplifier [37]. Although chromium doped laser materials have broad enough gain bandwidth for femtosecond pulses generation the chromium regenerative amplifiers are not effective because of thermal quenching of the fluorescence and short fluorescence time (Cr:YAG - 0,003 ms, Cr:LiSAF - 0,067 ms). Neodymium doped materials have four-level energy structure and high absorption and emission cress sections and they also have longer fluorescence time (Nd:YAG - 0.23, Nd:glass - 0.29-0.39 ms) than chromium doped materials. 11 ps pulses at 2.7 W average power were generated by Nd^{3+}:YVO4 laser [38]. 130 fs pulses were generated by Nd:glass laser with an antiresonant Fabri-Pero saturable absorber [39]. 64 fs pulses were generated with Kerr lens mode-locked Nd:glass laser, although average power was only 50 mW and it was pumped by Ti:sapphire laser [40]. Nd:glasses have broad enough gain bandwidth for the generation of femtosecond pulses, but the maximum average power is low due to its low thermal conductivity (~14 times lower than Nd:YAG) and high quantum defect. Nd:KGW and Nd:YAG laser materials have higher thermal conductivity than glasses do although their gain bandwidth is not sufficient for femtosecond pulse generation. The low quantum defect of ytterbium doped laser materials is one of the main advantages for the development of high average power lasers. 240 fs pulses at 22 W average power were generated by thin-disk Yb:KYW laser [41], 65 μJ pulses were amplified by Yb:KYW regenerative amplifier [42]. 44 μJ [43] and more than 100 μJ [44] pulses were generated by Yb:KGW regenerative amplifiers. Furthermore, lots of ytterbium doped laser materials have broad enough gain bandwidth for the generation of femtosecond pulses. 69 fs pulses were generated by Yb:BOYS laser with SESAM mirror [45]. 112 fs [46] and 230 fs [44] pulses were generated by Yb:KGW lasers and 101 fs [47] pulses were generated by Yb:KYW laser with a SESAM mirrors as well. 71 fs pulses were generated by Kerr lens mode locked Yb:KYW laser [48].

The analysis of the energy level structure of different laser materials reveals deeper understanding about the advantages of ytterbium-doped laser materials usage for high power lasers.

Three, four and quasi-three-level systems

The energy level system of most laser materials can be ascribed to three basic models (see Fig.2), where red arrows show non-radiative transfers and black arrows shows radiative transfers.

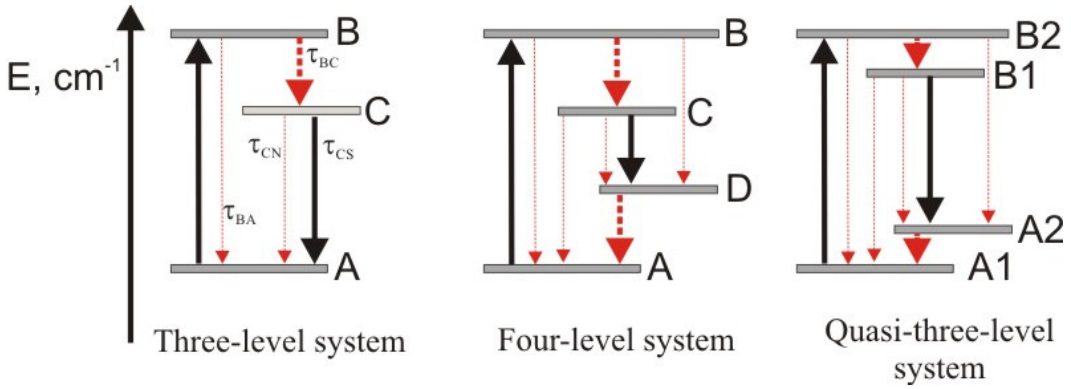

Fig.2. Energy level structure of three, four and quasi-three-level systems.

Three-level system

The ruby laser, Cr^{3+}:Al_2O_3, is a three-level system. In a three-level system, the laser transition ends on the ground state which makes it necessary to pump the crystal at high intensity to achieve at least the inversion $\Delta N > 0$, where $\Delta N = N_C - N_A$, where N_C is the population of the C level and N_A is the population of the A level. The population of the C level is negligible because of very fast non-radiative transition (from 10^{-8} s to 10^{-11} s) [30] to the upper laser level B in comparison with the B level lifetime (from 10^{-5} s to 10^{-3} s) [30]. Thus, the inversion can be achieved only when more than a half of ions are pumped into the upper laser level. The rate equation for a three-level system can be expressed as follows:

$$\frac{d\Delta N}{dt} = 2W_{AB}N_A - \frac{N_T + \Delta N}{\tau} - 2W_{CA}\Delta N\,, \qquad (1.1)$$

where τ is the lifetime of the upper laser level, N_T is the total system population and W_{xy} is the possibility of the radiative transition between X and Y levels and it can be expressed as follows:

$$W_{xy} = \frac{\sigma I_{xy}}{h\nu_{xy}}\,, \qquad (1.2)$$

where xy is the index showing the transition between X and Y levels, σ is the transition cross section, I_{xy} is the intensity of ν_{xy} frequency radiance.

Four-level system

The Nd:YAG laser is a four-level system. The main difference of four-level system from a three-level system is that the laser transition ends on the level well above the ground state which makes it easier to pump the crystal to achieve the inversion $\Delta N = N_C - N_D$, where N_C is the population of the C level and N_D is the population of the D level. The population of D level N_D depends on how close it is to the ground state:

$$N_D = N_A \exp\left(\frac{-\Delta E}{kT}\right), \qquad (1.3)$$

where N_A is the population of the ground A level, ΔE is the energy difference between A and D levels, k is Boltzmann constant and T is the temperature. The population of the Nd:YAG lower laser level in thermodynamic equilibrium at room temperature is less than 1% in comparison with ground state population. Thus we can assume that $\Delta N = N_C$ and the rate equation of four-level system can be expressed as follows:

$$\frac{d\Delta N}{dt} = W_{AB} N_A - \frac{\Delta N}{\tau} - W_{CD}\Delta N\,. \qquad (1.4)$$

Quasi-three-level system

The Yb:YAG laser is the most noteworthy quasi-three-level system. Ytterbium doped laser materials have a simple energy structure of two-manifold split into two groups of Stark levels, thus the laser transition ends on the level which is so close to the ground state that an appreciable population in that level occurs in thermal equilibrium at the operating temperature. The Boltzmann population factor shows the population of each Stark level in the manifold and may be expressed as follows:

$$f_{Ai,Bi} = \frac{\exp\left(-E_{Ai,Bi}/kT\right)}{Z_{A,B}}, \qquad (1.5)$$

where

$$Z_{A,B} = \sum^{Ai,Bi} \exp\left(-E_{Ai,Bi}/kT\right). \qquad (1.6)$$

f_{Ai} is the Boltzmann population factor for i level in A manifold, E_{Ai} is the i level energy and kT is the thermal energy. Thus the population inversion

$$\Delta N_L = f_{Bi} N_B - f_{Ai} N_A , \qquad (1.6)$$

where f_{Ai} and f_{Bi} are the Boltzmann population factors for lower and upper laser levels, N_A and N_B is the population of the A and B manifolds. Thus the rate equation for quasi-three-level system can be expressed as follows:

$$\frac{d\Delta N_L}{dt} = \left(N_t \left(f_{AK} f_{BL} - f_{AL} f_{BK}\right) - \Delta N_L \left(f_{AK} + f_{BK}\right)\right) W_K - \frac{\Delta N_L + f_{AL} N_t}{\tau} - \left(f_{AL} + f_{BL}\right) \Delta N_L W_L . \quad (1.7)$$

The comparison of three, four and quasi-three-levels systems

The main disadvantage of three-level system is that it requires pumping more than a half of population to achieve inversion and the unpumped gain medium exhibits strong absorption of the laser transition. The four-level system doesn't exhibit absorption of the laser transition because of negligible population of lower-laser level. On the other hand, the larger energy gap between the lower laser level and the ground level in a four-level system the more energy is transferred to a lattice due to quantum defect and it heats the gain medium. The efficiency of a quasi-three-level system depends on operating temperature. If the temperature of gain medium decreases the Boltzmann population factors f_{AK}, f_{BL} approache 1 and f_{BK}, f_{AL} approache 0. Thus, at lower temperatures the quantum efficiency of a quasi-three-level system approaches the quantum efficiency of a four-level system, but the optical-optical efficiency may become higher because of lower quantum defect. Cryogenically cooled Yb:YAG laser reaches the optical-optical efficiency of 76% at 100 K [49], it is the maximum efficiency reachable by Nd:YAG laser pumped at 808 nm.

The comparison of ytterbium doped laser materials

The analysis of various ytterbium doped laser materials was performed according to the main parameters shown in Table 1.

The gain bandwidth is the main parameter which determines how much short pulses are supported by the gain medium. The FWHM bandwidth of 100 fs Gaussian shape pulse at 1 μm central wavelength is 15 nm. However, the gain bandwidth

of 15 nm at FWHM is not sufficient to support such pulses because of effects like self-phase modulation [50], dispersion [51], gain narrowing [52] and gain shifting [52].

The lifetime of the upper laser level determines the energy storage of the amplifiers and the pump saturation intensity $I_{sot} = \frac{h\nu}{\sigma_a \tau \left(f_{AK} + f_{BK} \right)}$, where σ_a is the absorption cross section, $h\nu$ is the pump photon energy, τ is the upper laser level lifetime and f_{AK}, f_{BK} is the Boltzmann population factors of lower and upper pump levels.

The emission cross section and the absorption cross section determine the efficiency of amplification and pump absorption.

The quantum defects show what part of absorbed pump energy is transferred to the gain medium lattice due to the nonradiative transition. The low quantum defect and high thermal conductivity are especially important for the development of high average power lasers.

Thermally induced depolarization is suppressed if the gain medium has a sufficiently strong natural birefringence, so that the birefringent axis can not be significantly rotated by thermal effects. Thus, Yb:KGW is one of the most suitable medium for the construction of the femstosecond high output power laser system due to its natural birefringence, low quantum defect, broad emission bandwidth, absorption spectrum which is well matching the emission spectrum of commercially available high power laser diodes and good thermal conductivity.

Gain medium	Δλ (nm)	τ (ms)	σ_a (10^{-20}cm^2)	σ_e (10^{-20}cm^2)	q (%)	TK (W/mK)
Yb:LSB [53], [54], [55]	40	1,7	0,98	0,13 0,28	~5,8	2,8*
Yb:YCOB [53], [56], [57]	45 44	2,65 2,28	0,94 1	0,10 0,55 0,33	~10 ~5,2	4,7 2,1*
Yb:YAG [57], [58]	 8,5	1 0,95	0,8 0,82	2,2 2,1	~8,8	11-14
Yb:SFAP [53], [57]	4,1 4	 1,3	 8,6	 7,30	~13,5	 2*
Yb:KGW [59], [60]	20 25	0,8	12	2,8	~4,8	3,3
Yb:KYW [59], [60]	16 24	0,7	13	3	~5,7	3,3
Yb:YLF [57]	12	2,2	0,9	0,8	~7	6*
Yb: Sc_2O_3 [57], [61]	20 11,6	0,65 0,8	4,4	1,3 1,4	~6,4	15,5* 16,5
Yb:YAB [57]	20	0,68	3,4	0,8	~5,4	3*
Yb: LuAG [57]	16	0,925	0,75	2,7	~10	12,6*
Yb:NaGdW [62], [63]	33	0,32 0,397	1,51 1,21	-	~5	-
Yb:GdCOB [64], [57]	44	2,44	1,12	0,46 0,36	~7	2,1
Yb:BOYS [60], [65]	60	1,1	0,8	0,3	~7,5	1,5 1,8
Yb:CaBOYS [65]	50	1,2	0,6	0,3	~7,5	1,2
Yb:YSAG [58], [66]	12,5	1,1	0,7	1,42	~8,6	6,6
Yb:LAG [58]	6,5	0,51	0,7	3	~8,8	8
Yb:GGG [58]	12	0,8	0,46	2	~8,2	8
Yb:Y_2O_3 [58], [61]	12,2 14,5	0,85	0,24	0,98 1,06	~5,3	11 13,6
Yb:Lu_2O_3 [58], [61]	11,5 13	0,82	0,3	1,1 1,28	~5,4	12,5
Yb:stiklas [58]	52	0,8	2,6	0,64	~5,1	0,6

1.1 Table. Parameters of various ytterbium doped gain mediums

Spectroscopic properties of Yb:KGW crystal

The absorption and emission spectrum of 5% doped Yb:KGW at room temperature is shown in fig.3. Ella, Ellb and Ellc show the crystal orientation with regard to the way the crystallographic axis of the crystal matches the vector of electric field.

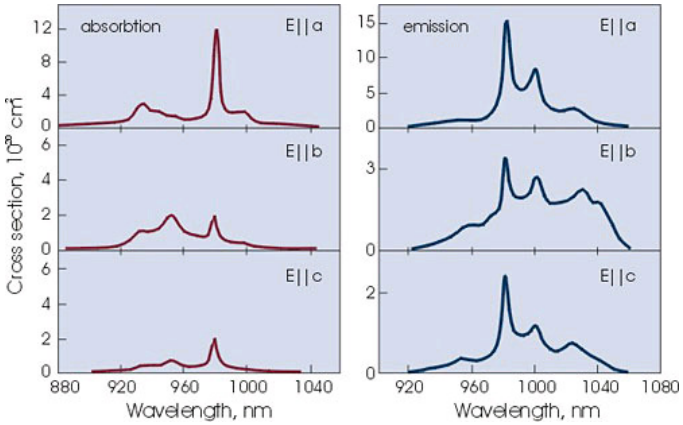

Fig.3. Absorption and emission spectra of 5% Yb:GKW

Although the emission bandwidth is broader for Ellb orientated crystal than that for Ella orientated crystal, the absorption cross section at 981 nm wavelength is 6.4 times and at 936 nm wavelength is two times higher for Ella orientated crystal than for Ellb orientated crystal, therefore the pump saturation intensity for Ella orientated crystal at 981 nm wavelength is 3.2 kW/cm^2 and it is ~6.3 times lower than pump saturation intensity for Ellb. For the pumping of 936 nm wavelength the saturation intensity for Ella orientated crystal is 31.5 kW/cm^2 whereas for Ellb orientated crystal it is 63 kW/cm^2.

2. Modeling of the laser cavity

A resonator is one of the main parts of the laser. Commonly it is a system of mirrors which creates the feedback by reflecting the light amplified by the laser. The resonator needs to be stable to create the proper feedback. It means that the beam should match it self after some round trips in the cavity.

The amplified beam quality depends on its spatial mode. The Gaussian beam has the best beam quality. The beam divergence of higher order spatial modes is higher, thus by applying spatial filters it is possible to suppress higher order spatial modes. The pump beam itself can be used as a soft aperture in the laser medium for the end pumped lasers especially if the laser medium with strong reabsorption is used. Therefore, for modeling of the laser cavity it is required not only to find stable cavity conditions but also to find properties of generated Gaussian beam.

In this part of the study main tasks were as follows:

1. To match pumping and generation spatial modes;
2. To find a proper laser resonator with the proper radiation intensity and energy fluence not damaging intracavity optical components;
3. To find proper position of the active medium so that the beam radius in the active medium is less dependent on the thermo-lens focal length;
4. The length of regenerative amplifier should be long enough so that the Pockels cell could completely change its state after the high voltage appliance and all acoustic ringing could be suppressed after one round trip in the cavity.

The form of the active medium

Because of quantum defect some part of pump power is converted into heat. The higher pump power the more heat is produced in the active medium and effective heat removal is needed. In order to improve the heat removal the ratio of the active medium surface and volume should be increased. However, even if the heat removal is efficient the thermo-optical phenomenon remains the limiting factor of maximum average power. Depending on the pumping and generation beams, the cooling scheme and the active medium properties the temperature gradient is induced in the active

medium (Fig.4). The refractive index of the matter depends on temperature, so the temperature gradient in the active medium is followed by refractive index gradient and this is how active medium influences the stability of a laser cavity.

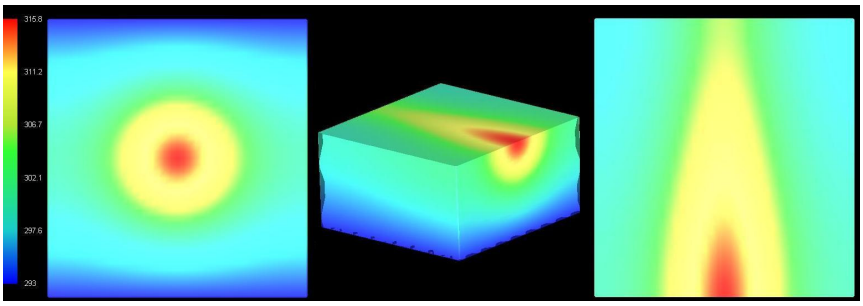

Fig.4. Example of the temperature distribution in the end-pumped cubic gain medium with a two cooled surfaces

There are two different concepts of the active medium design created to reduce the thermo-optical phenomenon. They are fiber [67] and thin disk [68] designs and both of them have some disadvantages for femtosecond pulse generation and amplification.

The single mode fiber maintains the Gaussian beam profile. However, the maximum core diameter of the single-mode fiber for ~1 μnm wavelength and the top-hat refractive index profile is ~30 μm [69]. The small beam spot size which leads to the high light intensity which together with long active medium length results in the low threshold of nonlinear effects. On the contrary, thin disk gain medium contributes only a small amount of nonlinearity, due to its small thickness (in order of few hundred micrometers [70, 71]) and the large mode size of the laser beam. However, small thickness of the gain medium leads to a small gain, thus to extract stored energy it is required a large number of resonator round trips which lead to strong gain narrowing. The increased amplification of spontaneous emission (ASE) for larger disks reduces the inversion and limits the scalability of thin disk lasers. The ASE in a fiber lasers not only reduces inversion but decreases temporal contrast of ultrashort laser pulse as well.

A bulk gain medium is a kind of intermediate situation, where longitudinal dimensions are in the same order as transverse dimensions, thus it has a higher gain in comparison to a thin disk gain medium and lower contribution to nonlinearity in

comparison to a fiber laser. However, a laser cavity with a bulk gain medium requires optimization in order to reduce thermal-lens influence on the resonator stability.

Analysis of the cavity stability

The thermal lens of less than 100 mm focal length is induced in Yb:KGW slab element pumped by more than 10 W pump power [71]. The main interest is how to minimize the effect of thermal lens induced in the laser crystal for the stability of the cavity. The well known ABCD matrix formulation is used for the analysis of the cavity and Gaussian beam propagation through the optical system. The four-mirror Z-shaped cavity has been analyzed. Figure 5 shows how the beam radius in the laser crystal depends on the focal length of the lens placed in the middle of the crystal and its position along the beam waste in the cavity without thermo lens. Any changes in the generation beam size changes its overlap with a pump beam. If laser beam radius increases the beam will suffer higher losses due to reabsorption in the unpumped laser crystal and if the laser beam radius decreases the optical-optical efficiency decreases as well.

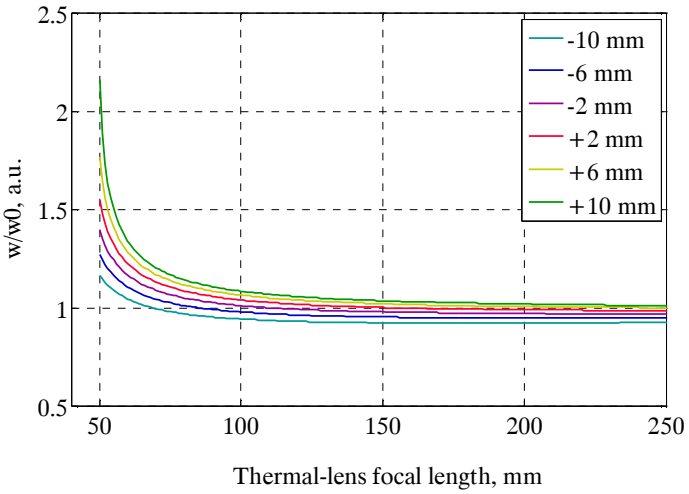

Fig.5. Laser beam waist radius versus thermal-lens focal length for various positions of gain medium along the laser beam waist in the cavity, were w is the beam radius at the gain medium and w_0 is the beam waist radius.

Two similar cavities have been compared with regard to beam radius in the gain medium dependence on the thermal-lens focal length (see Fig.6).

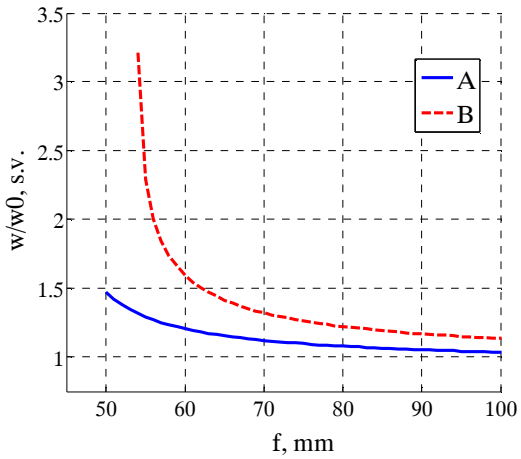

Fig.6.The beam radius versus focal length of the lens placed in the middle of a laser crystal in two similar cavities.

The beam radius in the laser crystal without thermal-lens is almost the same for both cavities but different curvature mirrors and different distances were used. The cavity B (see Fig.6) is more sensitive to the thermal-lens and its output power saturates at lower pump power then that for cavity A (see Fig.7).

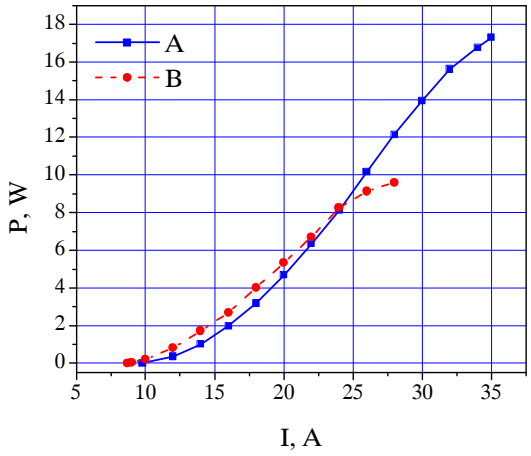

Fig.7. Output power versus pump current

Cavity with the nonlinear Kerr element

Nonlinearity is typically observed at very high light intensities. The simplest of nonlinear effects is the Kerr effect, which can be described as a change in the refractive index in proportion to the optical intensity *I*, thus the refractive index:

$$n(\vec{r},t) = n_0(\vec{r},t) + \Delta n\left[I(\vec{r},t)\right], \qquad (2.1)$$

Where n_0 is the linear refractive index and Δn is a change in refractive index induced by I. The Gaussian beam results in a Gaussian refractive index profile, similar to that of a gradient-index lens and the focal length of Kerr lens can be found from the equation:

$$f = \frac{n_0 w^2}{4 n_2' I_0 L}, \qquad (2.2)$$

where w is the beam radius, L is the length of the Kerr medium and n_2 is nonlinear refractive index. Since n_2 is positive in most materials, the refractive index becomes larger in the areas where the intensity is higher, usually at the centre of a beam, creating a focusing density profile which potentially leads to the collapse of a the beam itself. Such self-focusing effect can occur when the optical power is above the critical power:

$$P_c = \frac{c\varepsilon_0 \lambda^2}{2\pi n_2}. \qquad (2.3)$$

If the beam goes through the Kerr medium and then after some distance through the aperture, then its losses depend on the beam power, the more powerful beam the lower losses it will suffer. In this case it is possible to find the place for an aperture in the cavity where the beam radius decreases when the beam power increases accordingly, this is how Kerr lens mode locking with a hard aperture works. The parameter

$$\delta = \left(\frac{1}{w} \frac{dw}{dP} \right)_{P=0} \qquad (2.4)$$

shows how the beam radius is sensitive to a small power change at low power levels, the more sensitive it is the easier Kerr lens mode locking starts. The ABCD matrix for Kerr medium is deduced in paper [72].

Four-mirror resonator

Two spherical mirrors (ROC=150 mm) separated by the distance $Z = X + d + X_2$ (see Fig.7) have been used to focus beam into the gain medium and two plain mirrors at distances $L_1 = L_2 = 850$ have been used to end the resonator. The given four-mirror resonator has two stability zones and in the case of symmetric resonator ($R_1 = R_2$, $L_1 = L_2$) both zones are merged into one zone.

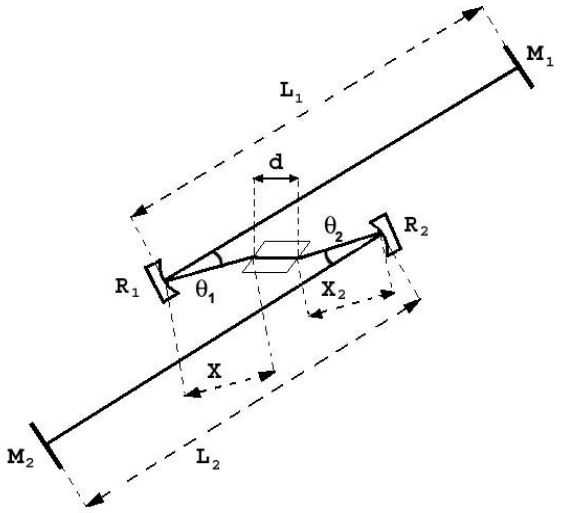

Fig.7. Four-mirror Z-shaped cavity

The map of δ parameter on a plain of M_1 mirror (see Fig.8) has been calculated by using ABCD formulation. There are two areas with a negative δ parameter, both are close to the stability limit of its resonator (see Fig.8). The beam mode size distribution in both stability zones with a negative δ value is almost the same because they are close to each other. However, if the intracavity power increases then the beam size change in a different stability zone is opposite.

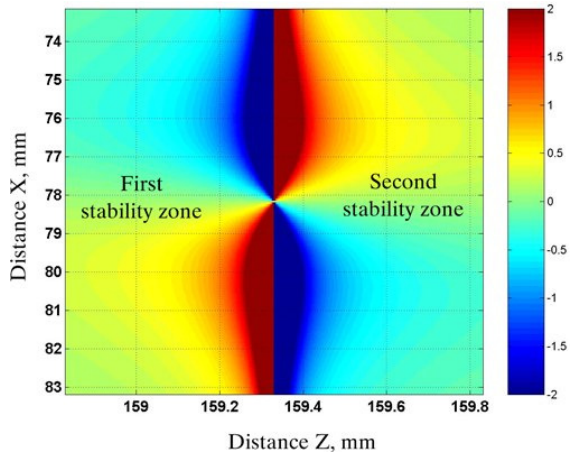

Fig.8. The map of δ parameter on a plain of M_1 mirror.

The change in the size of laser beam in the gain medium determines in which stability zone the pump beam operates as a soft aperture. The laser beam radius dependence on intracavity power is shown in Fig.9.

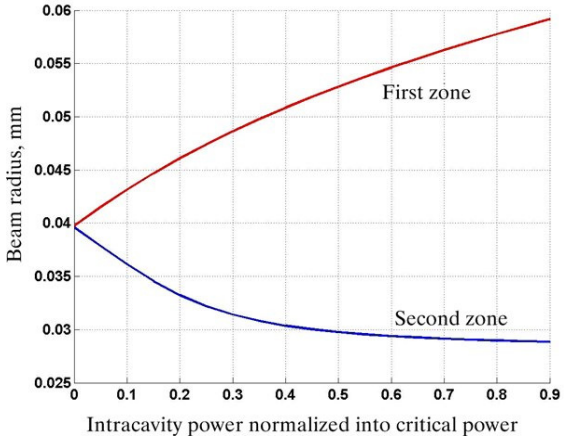

Fig.9. Beam radius versus intracavity beam power

3. Femstosecond Yb:KGW oscillator

Mode-locking

The laser may generate a number of longitudinal modes, $m = \Theta / \Delta\nu$ where Θ is the gain bandwidth and $\Delta\nu = c/2L$, where L is the length of the cavity. If each mode instead of oscillating independently operates with a fixed phase between it and the other modes, the modes of the laser will all constructively interfere with one another periodically, producing a pulse. The more modes there are in the phase the shorter and more powerful pulse is. The operation of the laser depends on its gain-loss dynamics. The most common method is to increase losses for low intensity light by incorporating a saturable absorber with suitable properties into the laser resonator. Any random number of modes present in the phase can create a fluctuation intensive enough to saturate the absorber, thus the net gain for this fluctuation will increase and the fluctuation will evolve into a pulse. The pulse duration could be determinated by the recovery time of the saturable absorber which forms the gain window. However, the lasers using semiconductor saturable absorber mirrors SESAM which very often have much longer recovery times than the shortest pulses generated from the given laser were demonstrated [73]. One reason for this behavior has been traced back to the soliton-like pulse formation, i.e., negative group delay dispersion (GDD) and self-phase modulation (SPM), occurring in femtosecond solid-state lasers. The soliton-like pulse formation leads to stable pulsing even in the presence of a considerable open net gain window following the pulse. The pulse is not any longer shaped dominantly by the saturable absorber, but the absorber is still essential for pulse stability.

The Kerr lens may be used as artificial saturable absorber but it needs a specific and precise cavity design. ABCD matrix formulation is used to optimize the cavity for Kerr lens mode locking [72, 74].

Mode-locking by SESAM mirrors

There are many designs of semiconductor saturable absorbers mirrors. The key parts are the Bragg reflector and the saturable absorber on it. Additional coatings are used to increase or decrease reflection from the input surface. The advantage of

semiconductor saturable absorbers is that the relevant absorber parameters can be varied by several orders of magnitude. The key parameters for a saturable absorber are its wavelength range (where it absorbs), its dynamic response (how fast it recovers), its saturation intensity and fluence (at what intensity or pulse energy density it saturates) and modulation depth (increase in reflectance when it is saturated). The saturation intensity can be expressed as following:

$$I_{sat,A} = \frac{h\nu}{\sigma_A T_A}, \qquad (3.1)$$

Where $h\nu$ is the energy of photon, σ_A is the absorption cross section and T_A is the recovery time. The recovery time of absorption depends on two processes, intraband thermal relaxation (10-100 fs) and recombination (from ps to ns). The saturation fluence is related to σ_A by the relation:

$$F_{sat,A} = \frac{h\nu}{m\sigma_A}, \qquad (3.2)$$

I.e. the saturation is reached when on average one photon with energy $h\nu$ impinges on a cross section area σ_A. Inside a linear cavity it may happen twice (m=2). In a ring cavity it may happen only once (m=1).

CW Mode-locking

In many applications we need the pulse sequence to be CW mode-locking instead of Q-switched mode-locking. From [75], the researchers came to the conclusion that the Q-switched mode-locking will be avoided if the following equation can be satisfied [75].

$$E_P^2 > E_{sat,L} E_{sat,A} \Delta R, \qquad (3.3)$$

where E_P is the intracavity pulse energy defined as intracavity average power divided by the pulse repetition rate, $E_{sat,L}$ is the saturation energy of the laser medium and it is proportional to $A_{eff,L}/\sigma_{e,L}$ where $A_{eff,L}$ is the average mode area inside the laser medium and $\sigma_{e,L}$ is the emission cross-section of gain material. $E_{sat,A}$ is the saturation energy of the absorber, which can be represented by $E_{sat,A} = F_{sat,A} A_{eff,A}$. $A_{eff,A}$ is the average mode

area inside the saturable absorber and ΔR is the modulation depth of the saturable absorber. Thus the critical pulse energy can be found.

$$E_{P,C} = \left(E_{sat,L} E_{sat,A} \Delta R\right)^{\frac{1}{2}} = \left(F_{sat,L} A_{aff,L} F_{sat,A} A_{eff,A} \Delta R\right)^{\frac{1}{2}}. \qquad (3.4)$$

If the intracavity pulse energy is higher than the critical pulse energy then the laser tends to operate as a CW mode-locked, else it operates as a Q-switched mode-locked.

Kerr lens mode-locking

The first Kerr lens mode-locked laser was demonstrated in 1991 [76], however the Kerr lens mode-locking mechanism was explained later [77, 78]. For a Gaussian beam, the Kerr effect focuses the radiation toward the center, and essentially an intensity-dependent graded-index lens is formed with the focal length depending on the power P.

$$f^{-1} = \frac{4 n_2 d}{\pi \omega^4} P, \qquad (3.5)$$

where n_2 is Kerr medium nonlinear refractive index, d is the length of Kerr medium and ω is the beam radius. The action of a fast saturable absorber can be achieved if an aperture is introduced in the resonator at a position where the mode size decreases due to increased intensity. The transformation of the power-dependent change in the spatial profile of the beam into an amplitude modulation is shown in Fig.10.

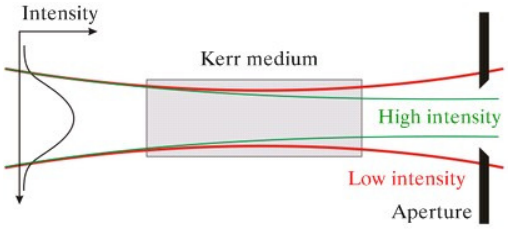

Fig.10. High intensity beam focusing in a Kerr medium

In case of a soft aperture the Kerr lens leads to a better overlap of the generation and the pump beam, and thus to a higher gain for the peak of the pulse.

As a beam has some spatial intensity profile the pulse has some time-dependent intensity profile and accordingly that the Kerr effect causes a time-dependent phase shift. Spectral broadening induced by self-phase modulation allows generating pulses with a broader spectrum than the gain bandwidth of the laser medium and thus the laser with the right dispersion balance in the cavity generates very short pulses. 12 fs

pulses were generated by Cr:LiSAF laser [79], 13,5 fs pulses were generated by Cr:LiSGaF laser [80], 61 fs pulses were generated by Yb:YVO_4 laser[81], 71 fs pulses were generated by Yb:KYW laser [48].

Dispersion compensation

The round-trip time in the resonator for all frequency components of the mode-locked pulse should be the same. Dispersion in the laser crystal and mirror coatings will result in different delay for different frequency components and thus temporal spreading of the pulse. A delay that is linear with frequency is called second order dispersion or group velocity dispersion (GVD). GVD is often quantified as the group delay dispersion GDD. Group delay dispersion in the Yb:KGW laser medium at ~1μm wavelength is positive and has flat dependence (see Fig.11), however, GDD in the mirror coatings may be complex.

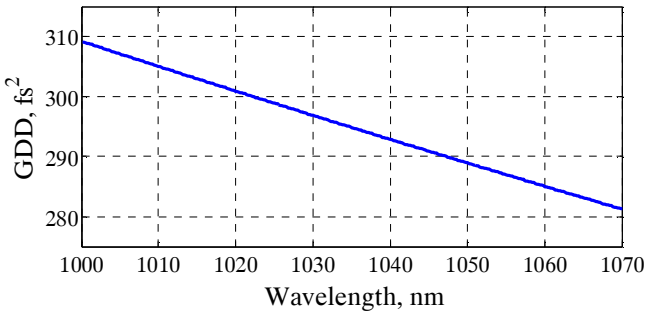

Fig.11. GDD curve of 2 mm length Yb:KGW crystal.

A number of devices may be used to compensate GDD in the laser cavity like the pair of prisms, Gires-Tournois interferometer or chirped mirrors.

Gires-Tournois interferometer

A Gires–Tournois interferometer (GTI) is an optical device designed for generating chromatic dispersion. It is a transparent plate with two reflecting surfaces, one of which has very high reflectivity, thus reflected beam interferes and has a phase shift that depends on the wavelength of the light. GDD of such device can be found from this equation.

$$GVD = -\frac{2\left(1-r^2\right)\sin\beta}{2r-\left(r^2+1\right)\cos\beta}\left(\left.\frac{d\beta}{d\omega}\right|_{\omega_0}\right)^2, \qquad (3.6)$$

where r is the first surface complex amplitude reflectivity ω is the angular frequency and the phase shift β can be expressed:

$$\beta = \frac{2dn\omega}{c}\cos\theta, \qquad (3.7)$$

where d is the distance between reflecting surfaces, n is the refractive index and θ is the angle of the beam incidence.

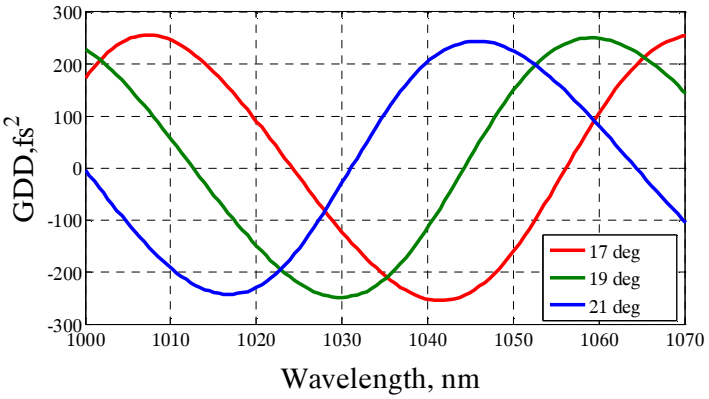

Fig.12. GDD curves of Gires-Tournois interferometer (2 μm thickness silica layer on a 100 % reflectance mirror) at different angles of beam incidence

The wavelength-dependent group delay dispersion of a GTI made of a 2-μm thick silica layer on a high reflector is illustrated in Fig.12.

Prism pair.

Pairs of prisms can be used for introducing negative dispersion into a laser resonator. The first prism spatially disperses the pulse, causing the long wavelength component to travel through more glass in the second prism than the shorter wavelength components do. The GDD of pair prism can be found from the following equation:

$$GVD \approx -4L\frac{\lambda_0^3}{2\pi c^2}\left(\left.\frac{dn}{d\lambda}\right|_{\lambda_0}\right)^2 + L_{prism}\frac{\lambda_0^3}{2\pi c^2}\left.\frac{d^2n}{d\lambda^2}\right|_{\lambda_0}, \qquad (3.8)\ [82]$$

where L is the distance between apexes of the prisms, λ is the wavelength, n is the refractive index and L_{prism} is the length of light path in the prism matter. Fig.13 shows the GDD curve of the 200 mm length prism (SF10 glass) compressor with a 4 mm length optical path inside prisms.

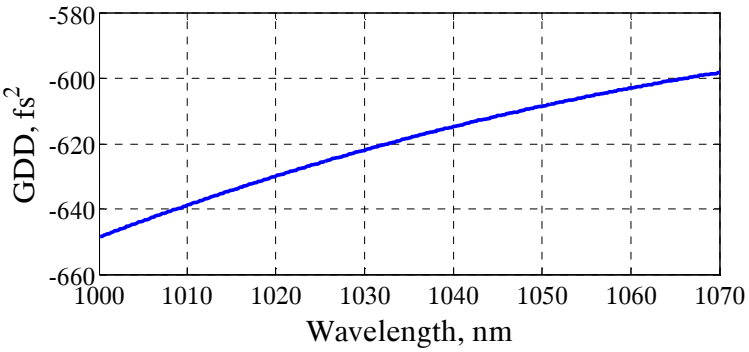

Fig.13. GDD curve of the prism compressor

Chirped mirrors

Chirped mirrors have multilayer coating with a dependence of the penetration depth of the incident optical field on a wavelength. Negative group delay dispersion is produced if the multilayer period is increased near the substrate so the optical path is longer for a longer wavelength. Although it is possible to create very complex multilayer coatings for compensation of higher order dispersion, but it requires very precise control over coating layers thickness.

CW Yb:KGW laser

Four-mirror Z-shaped cavity design (see Fig.14) has been used in this experiment with the aim to find the best matching of pump and generation beams in the laser medium which results in the best optical-optical efficiency.

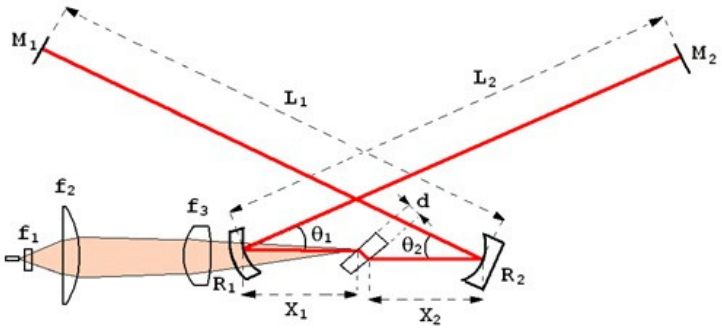

Fig.14. Diode pumped Yb:KGW laser scheme

The minimum pump beam diameter and thus the maximum pump intensity are limited by maximum output power of the laser diode and its beam quality. 5 W single emitter (1x100 μm) lased diode (Lumics GmbH) has been used to pump 1.2 mm length,

Brewster-cut E||a, 5% doped Yb:KGW crystal. The pump beam quality in its slow direction is $M^2_{slow} = 27$ and that in its fast direction is $M^2_{fast} \approx 1$. Thus the 60 μm diameter pump beam waist in the air (in the slow divergence plain) is ~0.2 mm length. In a laser crystal the pump beam waist is n times longer (where n is the refractive index of the laser medium) and for the pump beam upon incidence of Brewster angle the beam waist inside the laser crystal becomes ~2 times longer. The pump beam transmitting and generation beam reflecting spherical mirror (R1 mirror in Figure) with a radius of curvature ROC=75 mm has been used to match the pump and generation beams in the laser crystal. The laser crystal has been placed in the middle ($X_1 = X_2 = 38$ mm) between mirror R1 and another one spherical mirror with the same ROC. 100% (M1) and 99% (M2) reflectance mirrors have been used to end the resonator at distances of $L_1 = 680$ mm and $L_2 = 610$ mm, respectively. The generation beam diameter in the laser crystal is ~40 μm, thus ~1.5 times smaller than a pump beam. Under 2.7 W of incident pump power, the maximum output power reached 72 mW. Too low pump intensity, bad matching of pump and generation beams or not optimized reflectivity of the output mirror may cause low efficiency. The CW laser generation spectrum has peaks at 1032 nm and 1040 nm wavelengths. This means that the losses due to the reabsorption reduce the net gain at 1028 nm wavelength which according to the emission spectrum has the highest gain. Strong reabsorption is caused by low population inversion which in its turn results either from too low pump intensity or too high field intensity inside the cavity. The wedge partially inserted in the intracavity beam reduces the field intensity, but there were no major changes in the generation spectrum observed. Thus low optical-optical efficiency is caused by too low pump intensity and bad matching of pump and generation beams. The pump beam has been reshaped in order to improve its quality in slow axis. The laser pumped by reshaped beam ($M^2_G \approx 2.5$ and $M^2_L \approx 15$) provided up to 755 mW output power and reached 31% optical-optical efficiency.

SESAM mode-locked laser

SESAM mirror may be used as a passive mode-locker itself, or to initiate and stabilize mode-locking by other mechanism like Kerr lens. In this work we used BATOP GmbH mirror ($\Delta R_{1030} = 3\%$, $F_{sat,A} = 30\,\mu J/cm^2$, $\tau_A \leq 10$ ps). The experimental set-

up is shown in Fig.15, where $R_1 = R_2 = 200$ mm, $R_3 = 300$ mm, $d = 1.2$ mm, $L_1 = 460$ mm, $L_2 = 1200$ mm, $L_3 = 140$ mm, $X_1 = X_2 = 102$ mm, $\theta_1 = 12^0$, $\theta_2 = 8^0$, $\theta_3 = 6^0$ and the reflectivity of M_2 mirror is 2%.

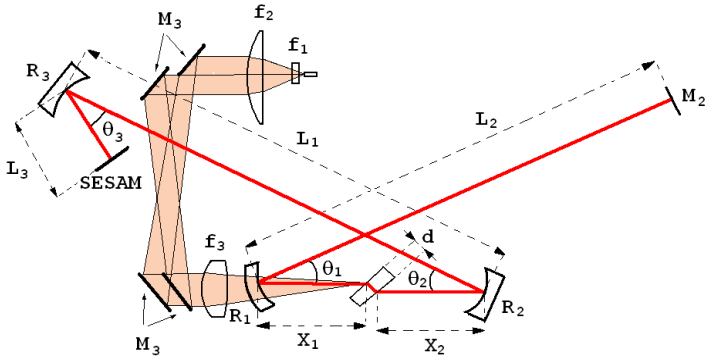

Fig.15. The scheme of diode pumped Yb:KGW laser with a SESAM mirror

The length of the cavity is 2 m long, thus the pulse repetition rate is 75MHz. The laser beam waist in the gain crystal was ~29 μm and that on SESAM mirror was ~60. Thus, according to (3.4) the CW mode locking should be reached at higher than ~220 mW output power. Fig.16 shows the laser behavior and measured output power dependence on the pump power. The CW mode locking is reached at above ~90 mW output power, the estimated output power was more than two times higher than that. Above the ~380 mW output power the laser tend to generate two pulses.

A pair of prisms has been used in order to compensate dispersion of the gain medium. The pulse duration was estimated according to the pulse bandwidth. The broadest pulse bandwidth ($\Delta\lambda = 6\ nm$) was observed in the presence of positive dispersion in the cavity.

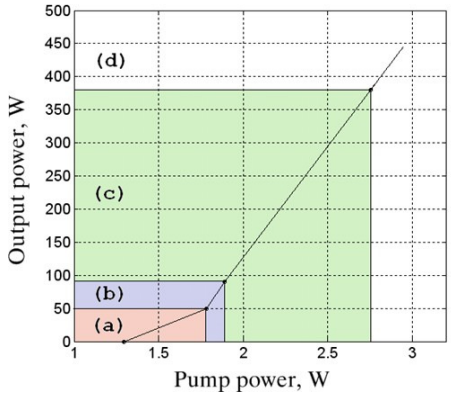

Fig.16. The output power versus pump power, (a) is the CW operation, (b) is the Q-switched mode locking, (c) is the CW mode locking and (d) is the mode locking with two pulses.

However, theoretical calculations and experiments show that the shortest pulses are generated by the lasers operating in a soliton mode locking in the presence of the negative dispertion in the cavity [83]. This disagreement is occurs because we estimated only the dispersion of the gain medium and the prism compressor, however, the mirror used to match pump and generation beams has complex dielectric coatings and it may create noticeable amount of negative dispersion. Thus the dispersion balance in the laser cavity without the prism compressor may be sufficient for the soliton mode locking. It explains the lower output power required for CW mode loking (see Fig.16).

The broadest obtained pulse bandwidth (6 nm) corresponds to ~ 250 fs bandwidth-limited pulse duration. For the further shortening of the pulse Kerr nonlinearity in the gain medium may be used. Fig.17 shows the map of δ parameter calculated at the plane of R_3 mirror (see Fig.15).

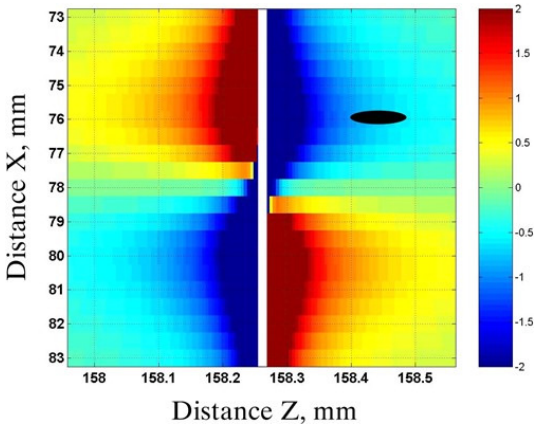

Fig.17. The map of δ parameter, black spot shows the working point for a given set-up cavity

1.5 times braoder pulse spectrum is observed with the apperture placed into the cavity near to R_3 mirror (see Fig.18). However, the pulse spectrum is shifted to longer wavelengths than that without an apperture. The wavelength-tuning curve (see Fig.18, green dots) shows that the gain medium supports a much braoder bandwidth. The high losses due to reabsorbtion in the unpumped gain medium may cause this behiviour.

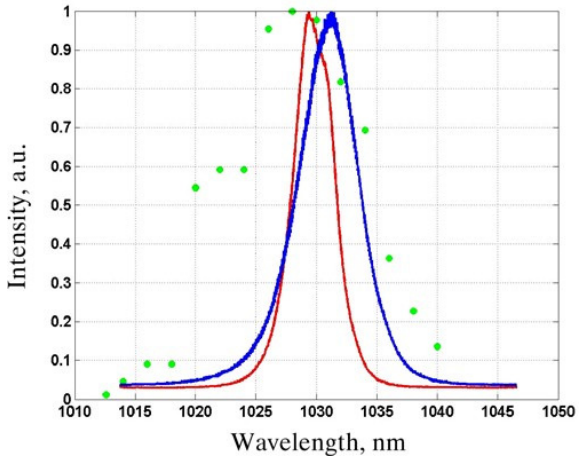

Fig.18. Pulse spectrum, (red) is the pulse spectrum produced by the laser without an aperture, (blue) is the pulse spectrum produced by laser with a apperture, green dots show the gain bandwidth

Further research on Kerr lens mode locked oscillator was done by using a new pump source (from UAB MGF „Šviesos konversija“) which contains 40 W diode bar and microoptics shaper producing pump beam with equal beam quality in slow and fast directions ($M^2 =\sim 35$). After the optimization of the resonator, the gain medium length and the prism commpressor the Kerr lens mode locking has been obtained and 31 fs pulses hasve been generated (see Fig.19). To our knowledge they are the shortest pulses reported from the laser with a bulk ytterbium doped gain medium.

The oscillator with a similar configuration and generating ~60 fs pulses was used for generation of terahertz radiation [84].

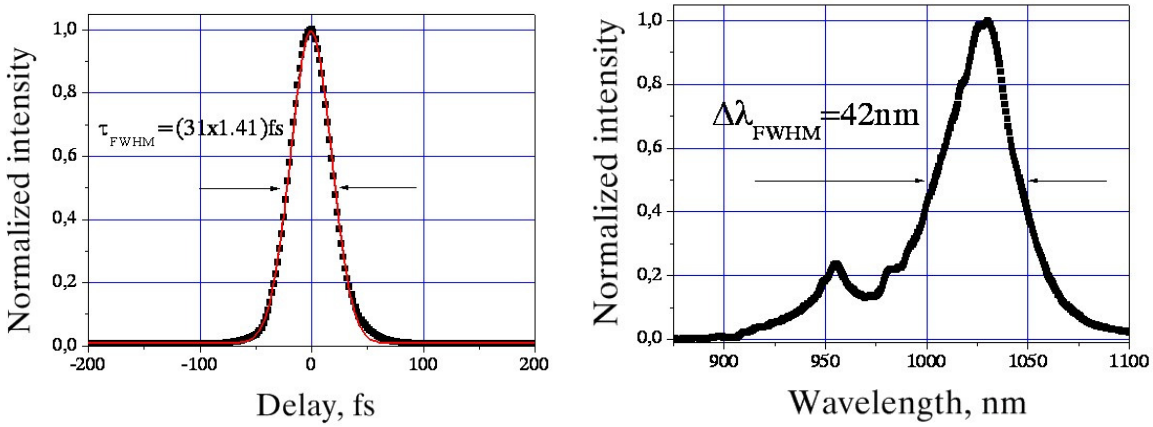

Fig.19. Autocorelation and spectrum of the 31 fs pulse.

4. Ultrashort pulse amplification

Efficient amplification of ultrashort pulses and energy scaling in compact diode pumped solid state lasers is limited by nonlinear effects due to the high intensity of the signal in the amplifier medium. This leads to the self-phase modulation, self-focusing, optical damage, and pulse breakup.

Chirped pulse amplification

The chirped pulse amplification laser dissects a laser pulse according to its frequency components, and reorders it into a time-stretched lower-peak-intensity pulse of the same energy. This benign pulse can then be amplified safely to high energy, and then only afterwards reconstituted as a very short pulse of enormous peak power. The scheme of CPA is shown in Fig.20.

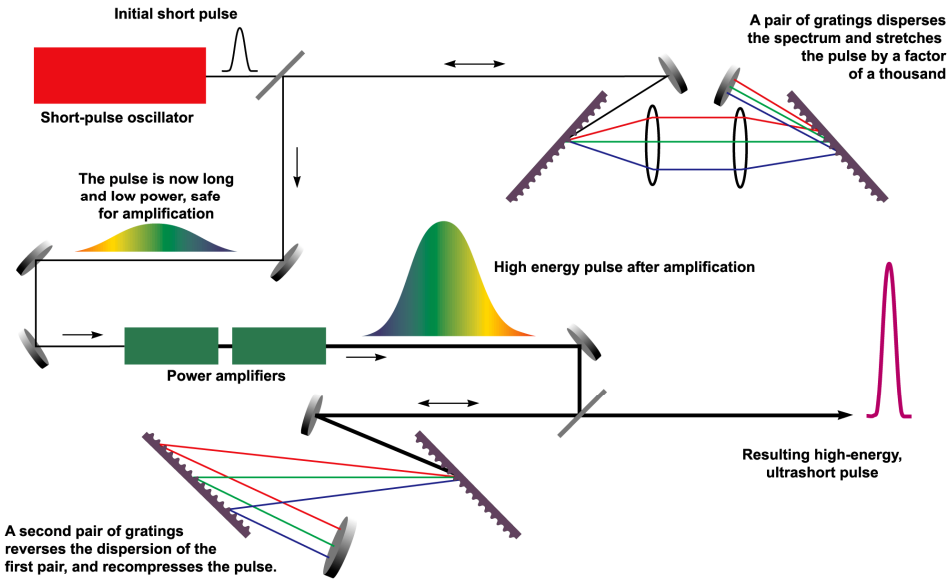

Fig.20. The scheme of chirped pulse amplification [85].

Tilted pulse amplification

For relatively narrow spectral bandwidth of the pulses the chirped pulse amplification CPA technique is not applicable for intensity reduction. An increase in the mode diameter in the amplifier medium leads to a decrease in both gain and efficiency of the amplifier. We have done an experimental demonstration of a novel method for stretching of picosecond pulses, which we call Tilted Pulse Amplification (TPA). We demonstrate reconstruction of a 15ps pulse after stretching to 200 ps and amplification

with a gain factor of 4.5. The idea of the pulse stretching is based on the pulse tilting after reflection from a diffraction grating (Fig.21). The layout resembles that of the pulse stretcher used in the traditional chirped pulse amplifiers (CPA), however the amplifier medium is placed in the focal plane of the image inverting telescope. At this position the pulse tilt angle becomes equal to 90^{o} and pulse duration here is defined by the diameter of the initial beam and the tilt angle, and does not depend on the initial duration of the pulse [86]. The pulse diffracted by the grating acquires a tilt defined by the incidence and diffraction angles.

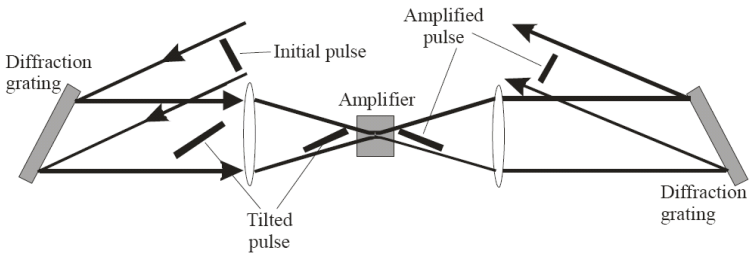

Fig.21. Principle of pulse stretching in the TPA

Simple geometrical considerations show, that in a particular case of Littrow configuration and Gaussian beam profile the pulse duration τ_{str} (FWHM) in the Fourier plane of the focusing spherical lens is determined by the beam size, wavelength and grating pitch:

$$\tau_{str} = \frac{\sqrt{2\ln 2}\, d \tan(\theta_{Littrow})}{c}, \qquad (4.1)$$

where d is the beam diameter (FWe^{-2}) on the grating, $\theta_{Littrow}$ is the Littrow angle, and c is the speed of light. For a beam diameter of d=20 mm and Littrow angle of $\theta_{Littrow}$=73 deg (an approximate value for 1064 nm wavelength and 1800 mm^{-1} grating), the pulse duration in the focal plane of the lens is τ_{str}=250 ps. Thus for a pulse duration of 10 ps a stretching factor of 25 can be achieved. One should note that the main limitation of this stretching method comes from the fact that the pulse remains stretched only within limited distance. This means that the image of the focal plane has to be relayed in case of multi-stage amplifiers, and makes the application to regenerative amplifiers impractical. Although the TPA design is almost identical to that of spatially dispersed amplifiers of ultrabroadband pulses [87-89], its potential for amplification of narrow bandwidth

picosecond pulses has been overlooked so far. It is also worth noting that the spatially dispersed amplifier requires certain linear dispersion to suppress the gain narrowing, whereas the duration of the stretched pulse in TPA case is ultimately determined by the spectral resolution of the dispersive optic. The set-up of the test experiment is schematically depicted in Fig.22. We used passively mode locked Nd:YVO4 oscillator emitting 15 ps pulses at 85 MHz repetition rate with 200 mW average power as the signal source for two-pass amplifier in TPA design. The amplifier medium was Nd:YAG (L=8 mm, diam=5 mm, NNd=1%) crystal longitudinally pumped by a single laser diode bar emitting up to 13 W at 808 nm in a shaped beam with M^2=45. For pulse tilting we used 1800 mm-1 diffraction grating in Littrow geometry. The focal length of the first lens (f1=500 mm) determines the dimensions of the signal beam in the amplifier crystal whereas the focal length of the second lens (f2=90 mm) sets the magnification of the telescope and thus the pulse stretching factor of the system.

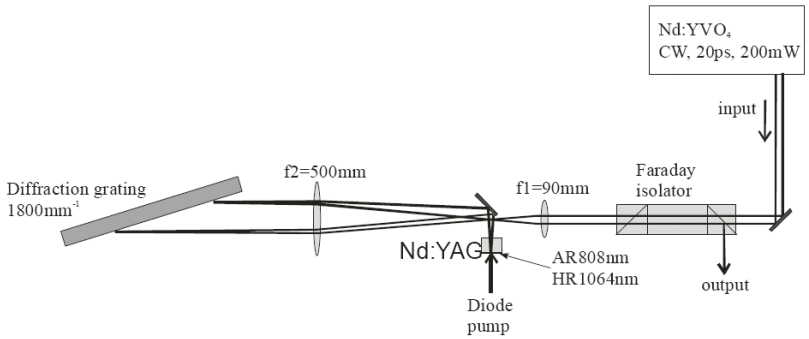

Fig.22. Experimental setup of the TPA. AR, antireflective; HR, highly reflective.

For separation of the amplified beam we used Faraday isolator since separation simply by geometry increased the numeric aperture of the system and caused strong spherical aberrations. The signal spot on the face of the amplifier crystal had elliptical shape with vertical and horizontal axis measuring 45 and 400⌈m respectively. The short axis of the ellipse corresponded to the waist of focused Gaussian beam whereas the long axis was determined by the bandwidth (0.14 nm) of the pulse and the linear dispersion of the system. The peak power of the signal pulses by far could not reach the threshold of the self modulation in the amplifier crystal even without stretching, however the use of continuous train was adequate for testing reconstruction of the pulse and the influence of thermal lensing. When continuous wave (CW) pump beam with

diameter of 200 μm was used, the duration of the amplified pulse was strongly influenced by the pump induced thermal lens in the Nd:YAG crystal. The thermal lens modifies the wave front of the spatially dispersed beam, which in turn changes the time delay between spectral components and prevents the pulse of being recompressed. By applying pulsed (QCW) pump (repetition rate 200 Hz, pulse duration 1 ms) we eliminated the thermal lens and achieved a gain factor of 4.5 in the double-pass scheme (Fig.23). However, in this case the duration of the amplified pulse (Fig.24a) was still impaired by spectral narrowing in the amplifier due to poor overlap of the spatially dispersed signal with the pump beam (signal, 45 μm ×400 μm, pump, 200 μm × 200 μm). With reshaped pump beam (170 μm × 700 μm) we observed good pulse reconstruction after amplification (Fig.24b), however at the expense of the gain drop to 1.7. The reconstructed pulse was still ~20% longer than the original one, presumably due to residual geometric aberrations in the optical scheme. As one can see, the thermal lensing is the main obstacle for achieving high average power as while preserving the pulse duration. Several options can be considered for improving the situation. A laser medium with higher gain cross section like Nd doped Vanadate crystal can be used which would require lower pump intensity. The use of a spherical or cylindrical lens in the vicinity of the amplifier crystal could improve the pulse reconstruction significantly if the aberrations of the thermal lens are insignificant. And finally, an aspheric optic with a refraction inverse to that of the thermal lens could lead to proper pulse reconstruction, however only within limited pump power range. It is interesting to note that thermal lensing in the amplifier crystal has a very similar effect on the reconstructed pulse shape as the phase self modulation has on the pulse shape using CPA technique. In turn, phase self modulation in TPA scheme would lead mainly to the beam distortion after reconstruction. As an additional benefit of the TPA method is suppression of the gain narrowing if the amplifier is driven in saturation [87-89]. On the other hand, the saturation by a single pulse would not lead to the distortion of the pulse spectrum as it might be in the case of CPA [90]. However in our case this saturation might lead to the distortion of the beam, since beam intensity profile is converted into the pulse shape in the amplifier. In contrast to CPA these distortions can be reduced by passing the amplifier once again with inverted beam.

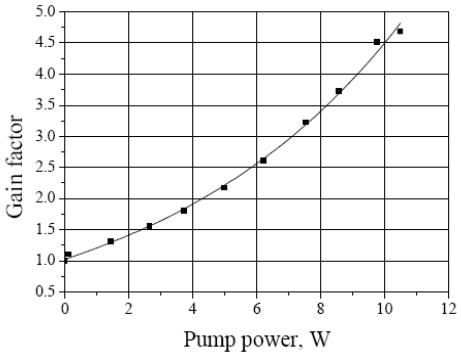

Fig.23. Gain of the TPA system versus pump power.

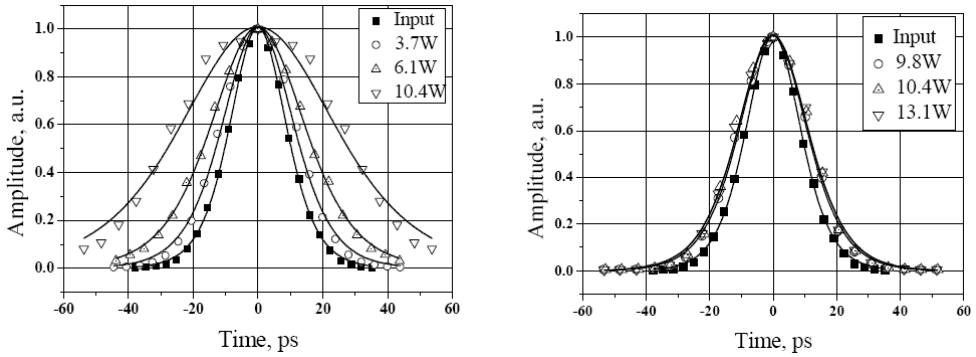

Fig.24. Autocorelation traces of the pulses amplified at different quasi-CW pump powers. (a) Signal beam 45 μm ×400 μm; pump beam 200 μm × 200 μm. (b); Reshaped pump beam 170 μm × 700 μm, signal beam 45 μm ×400 μm.

The dynamics of the regenerative amplifier

The principle scheme of the regenerative amplifier is shown in Fig.25. The Pockels cell inside the cavity controls the energy ejection out of the cavity. At the same time the Pockels cell modulates the quality value of the cavity. The regenerative amplifier resonator has been optimized on the basis of the results obtained from the examination of the thermal-lens effect on the stability of the resonator. 17 W CW output power is reached at 58 W pump power, it is 29% optical-optical efficiency.

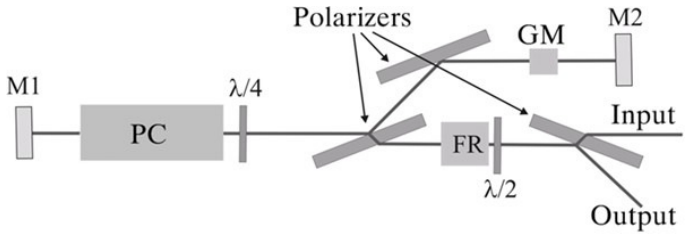

Fig.25. Principle scheme of the regenerative amplifier. PC is the Pockels cell, FR is the Faraday rotator, GM is the gain medium, and M1 and M2 are the resonator mirrors.

Although E||a absorption cross section is 6.4 times higher than that for E||b, the E||b emission cross section at 1040 nm wavelength is ~2 times higher than that for E||a. The reabsorption at 1040 nm is lower than the reabsorption at 1028 nm because the laser transition ends on the level with a lower Boltzmann population than that at 1028 nm. The numerical analysis of (1.7) equation has been used for modeling of the pulse amplification in the regenerative amplifier. The comparison of the maximum pulse energy in both cases (E||a and E||b orientated Yb:KGW crystal) is shown in Fig.26.

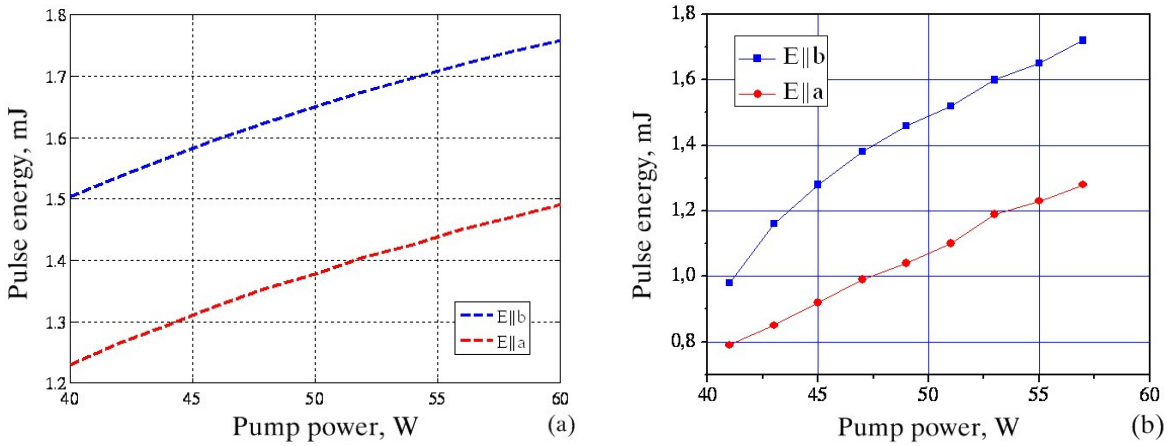

Fig.26. The pulse energy versus pump power. (a) Modeling results, (b) experimental results.

The maximum pulse energy for E||a configuration is higher than that for E||a configuration because it is easier to achieve the inversion for 1040 nm transition. However, the experimental results showed that the maximum pulse energy in E||b configuration decreases more than that for E||a configuration if pump power decreases. It is because we had limited pulse round trip number in the cavity (53 round trips) in the experimental setup and for E||b configuration it is not enough round trips to extract maximum stored energy due to lower gain than for E||a configuration. The higher pulse repetition rate the lower inversion in the gain medium is due to shorter pump time between amplified pulses. Thus at high repetition rates E||a configuration is more efficient than E||b configuration due to lower pulse round trip number which is needed to extract the maximum pulse energy (Fig.27).

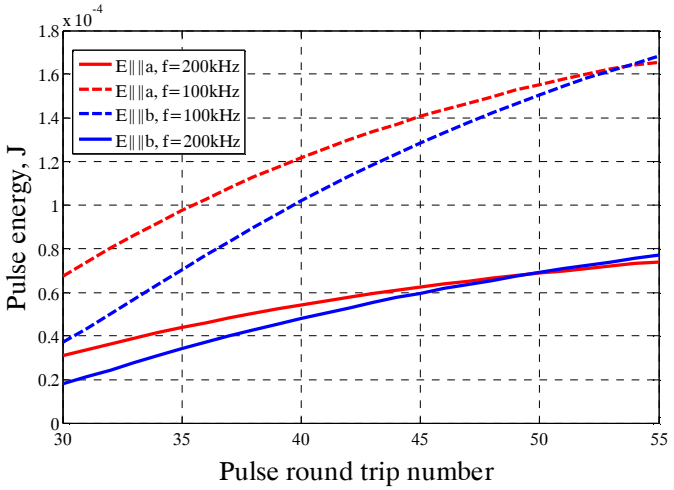

Fig.27. The pulse energy versus pulse round trip number in the amplifier cavity.

The modeling results reveal that under some conditions bistable pulse amplification occurs (Fig.28). It happens when reasonable part of stored energy remains in the gain medium after the pulse amplification and the pump is not intensive enough or the pump time is too short to restore the same inversion in the gain medium before the amplification of the next pulse.

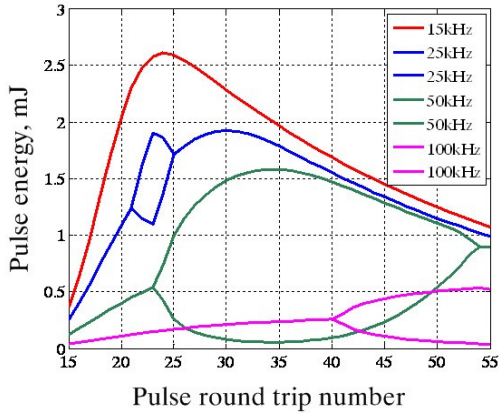

Fig.28. Calculated pulse energy dependence on the pulse round trip number in the cavity

In camparison with CW laser the optimal ytterbium doping level of the regenerative amplifier gain medium additionally depends on its pulse repetition rate. The higher pulse repetition rate the lower Yb doping level is required to reach the maximum pulse energy (Fig.29).

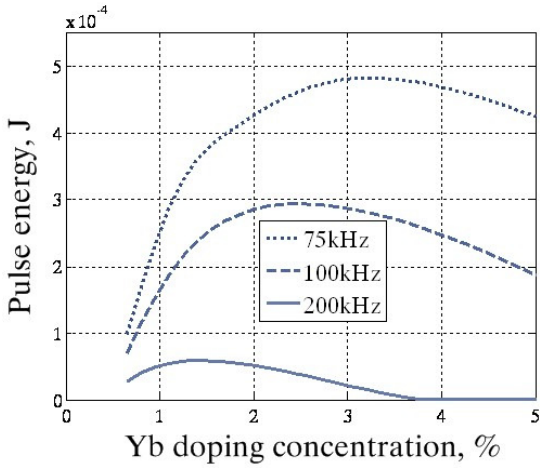

Fig.29. The maximum pulse energy versus Yb doping concentration of the gain medium at different pulse repetition rate

In the Fig.30 is shown the maximum pulse energy of 25 round trips amplifier cavity dependence on pulse repetition rate. The limiting factor of the maximum pulse energy at pulse repetition rates up to 5kHz for the given cavity is Raman scattering. At (8 kHz - 50 kHz) pulse repetition rates the pulse energy is limited by bistable amplification and for the higher than 50 kHz pulse repetition rates the pulse energy is limited due to limited average power which accordingly is limited by thermal-lens effect in the gain medium.

Fig.30 The maximum pulse energy of 25 round trips amplifier cavity dependence on pulse repetition rate.

Ultrafast pulse characterization in the time domain

Techniques for the complete measurement of ultrashort laser pulses are now well established. The most popular and simple way to characterize a pulse is the

measurement of autocorrelation function and the spectrum of a pulse. However this does not provide sufficient information for the complete characterization of the bandwidth non-limited pulses. Frequency resolved optical gating (FROG) [91], its modifications X-FROG [92] and GRENOUILLE, and spectral phase interferometry for direct electric-field reconstruction (SPIDER) are powerful techniques that precisely determine the pulse shape and phase information of a short pulse, which can not be obtained through autocorrelation. Although these methods can provide full amplitude and phase information they suffer either from phase ambiguity, complicated interferometric optical layout or sophisticated mathematical algorithms for processing of a signal. Alignment of modern chirped pulse amplification (CPA) systems requires straightforward and evident methods for ultrashort pulse measurement, which could provide truthful directions for optimization of pulse width. In this paper we present a novel method for characterization of ultrashort pulses with improved spectral resolution and extremely simple and straightforward data acquisition with no ambiguities. The new method differs from FROG in a way that spectral processing of a pulse is performed before non-linear interaction and spectral resolution is determined by the dispersion of a spectral instrument and is not influenced by the bandwidth of the pulse itself.

We used the new method for characterization of a Yb:KGW based femtosecond system which incorporates a transmission grating based stretcher and compressor in a traditional chirped pulse amplification (CPA) scheme. The setup of the experiment is schematically depicted in Fig.31.

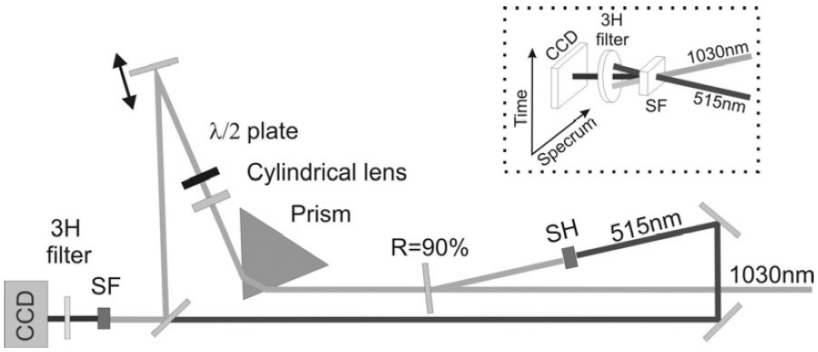

Fig.31. The optical scheme of the device for characterization of ultra-short pulses in the time domain. Inset shows in more details the interaction of the pulses in nonlinear medium. SF – represents BBO crystal for sum frequency generation, SH represents BBO crystal for second harmonic generation, 3H filter represents third harmonic filter.

The pulse under investigation from the laser is divided by a 10/90 beam splitter, 90% of light goes for the second harmonic generation as a probe pulse and 10% of light goes to the prism as a test pulse. In order to clean the probe pulse we generated the second harmonic using much lower than saturation intensity. An autocorrelation trace and the spectrum of the probe pulse are shown in Fig.32(a,b). For comparison, time-bandwidth product of the fundamental pulse was $\Delta\nu\Delta\tau$=0.81 and for the second harmonic pulse was $\Delta\nu\Delta\tau$ =0.58.

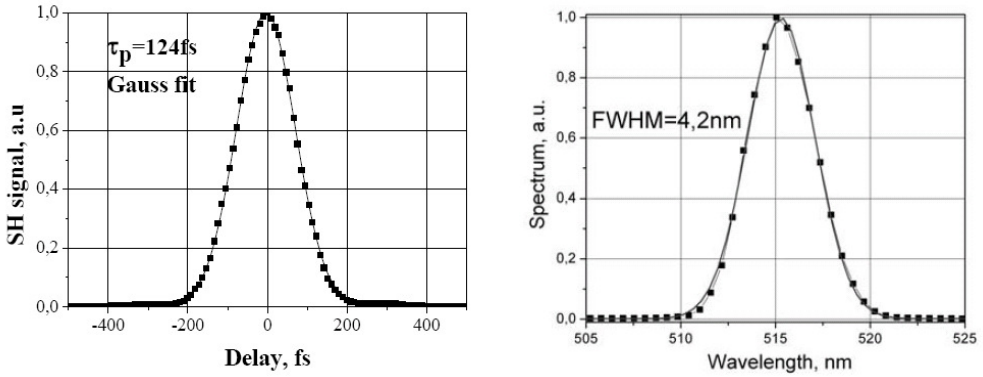

Fig.32. Autocorrelation function (a) and spectrum (b) of the second harmonics pulse used as a probe. The pulse duration was calculated using Gaussian fit, $\Delta\nu\Delta\tau$=0.58.

The remaining 10% of the pulse passes a Brewster type prism made of SF10 glass to achieve angular dispersion. The both pulses are combined in a thin nonlinear crystal for noncollinear sum frequency generation. The crystal is positioned in the focal plane of a cylindrical lens. We used a 1mm thick BBO crystal (θ=30deg), which provides sufficiently wide acceptance bandwith. λ/2 waveplate rotates the polarization of the pulse for Type-2 interaction.It is well known that after a dispersing prism the pulse acquires group velocity dispersion intrinsic for tilted pulses [93]. This effect slightly influences the result of the measurement, however, in practical CPA systems the group velocity dispersion can be simply compensated by detuning the compressor length. The dispersed first harmonic pulse and the second harmonic probe pulse are combined in the BBO crystal at about 10deg angle in the plane perpendicular to the plane of Fig.31 (see inset of Fig.31). Such a scheme allows single shot pulse characterization similarly to single shot autocorrelator [94] with added frequency resolution. A CCD camera behind the UV filter detects the sum frequency (third harmonic) image. Time scale is on the vertical axis of the image and frequency on the horizontal axis. A typical spectrally

resolved correlation image of the optical pulse is shown in Fig.33. The autocorrelation function and the spectrum of the same pulse is shown in Fig.34 (a,b). The gray line in Fig.34 indicates relative delay for different spectral components. This line was obtained by finding analog of the center of mass in each column of image matrix. Oscillations of this line show the presence of uncompensated high order dispersion (higher than 3-rd and 4-th order).

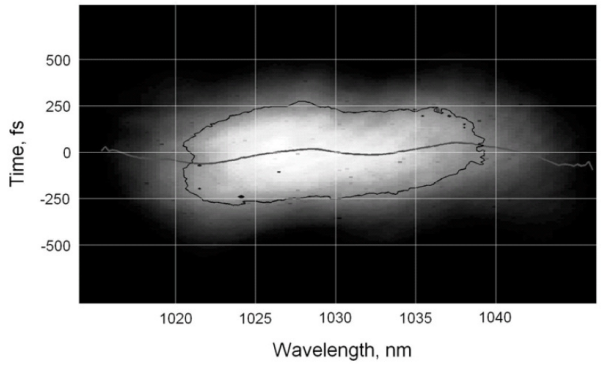

Fig.33. The typical spectrally resolved correlation image of an optical pulse.

The autocorrelation function and spectrum of the pulse is shown in Fig.35(a,b). The gray line indicates relative delay for different spectral components and the contour line shows half maximum level.

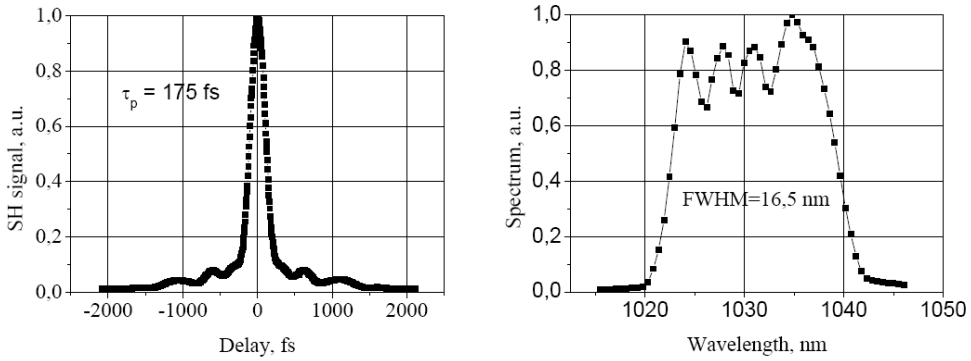

Fig.34. The autocorrelation function (a) and spectrum (b) of an optical pulse used for the demonstration of the new method (Fig.31).

We attributed this dispersion to imperfections of the surface quality of an acylindrical lens used in the stretcher. We measured these imperfections of the acylindrical lens using another technique too.

To demonstrate possibilities of the method we misaligned the stretcher and the compressor of the CPA system in such a way that third order (Fig.35a) or second order

dispersion (Fig.35b) dominated. It is interesting to note that the shown images were obtained without any sophisticated mathematical processing.

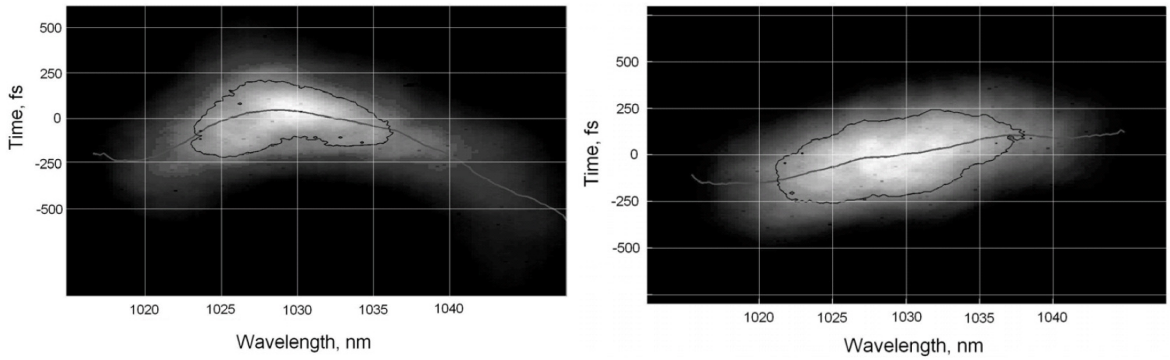

Fig.35. The spectrally resolved correlation image of the optical pulse with the strong third order dispersion chirp (a) and the second order dispersion chirp (b). The gray line indicates relative delay for different spectral components, and the black contour line shows half maximum level.

An interesting and distinguishing feature of the new method is enhanced spectral resolution. When two pulses, test and probe, interact in a nonlinear medium, the test pulse is spectrally resolved with a resolution defined by the resolution of a spectral instrument and the bandwidth of the probe pulse could not influence spectral resolution. In the case of FROG or XFROG the spectral resolution is blurred by the bandwidth or a pulse itself of by the bandwidth of a probe pulse and only phase and amplitude retrieval algorithms help to get complete information about a pulse.

The amplified pulse was compresed down to 148 fs (see Fig.36) after the replacment of problematic acilindrical lens into new one with a more uniform spherical surface and optimization of the stretcher.

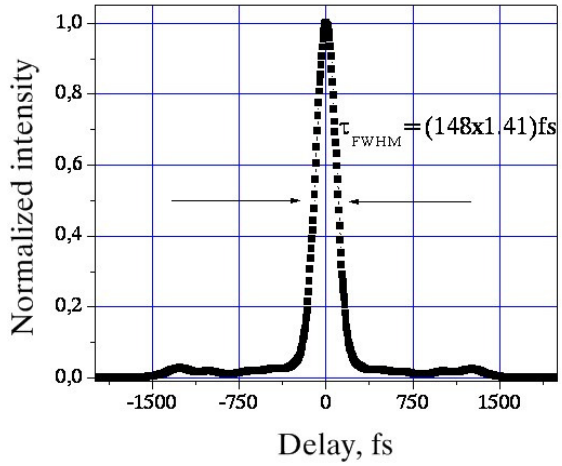

Fig.36. The Autocorelation function.

Conclusions

- On the basis of thermal-lens and nonlinear Kerr medium effect on the stability of the resonator study results we have demonstrated a Kerr lens mode-locked diode pumped Yb:KGW oscillator that generates 31 fs pulses. To our knowledge, this is the shortest pulse obtained from the laser based on ytterbium doped bulk gain medium.
- The study and optimization of cavity configuration, length, orientation and doping level of the gain medium has allowed to demonstrate that the gain bandwidth of the Yb:KGW regenerative amplifier is sufficient to support the amplification of the 150 fs pulses.
- Information obtained by the new design single shot autocorrelator with a spectrical resolution doesn't need complex algorithm to be unambiguously interpreted and is easy to use for optimization of CPA stretcher and compressor.
- It was experimentally demonstrated the amplification and reconstruction of a 15 ps pulse after stretching to 200 ps in the tilted pulse amplification (TPA) scheme. It has be found, that aberrations of focusing system can significantly distort the reconstructed pulse. A gain factor of 4.5 in a two-pass end pumped Nd:YAG amplifier has been achieved using quasi-CW pump and CW 15 ps pulse train as the seed. Similar gain factors with CW pump can only be achieved with proper management of thermal lensing in the amplifier medium.
- The diode pumped Yb:KGW femstosecond laser system consisting of a Kerr lens mode locked oscillator and the regenerative amplifier has been demonstrated for pumping of the optical parametric amplifiers, two-photon polymerization, generation of terahertz radiation and micro-processing of different materials.

References

1. Maiman, T.H., *Stimulated Optical Radiation in Ruby.* Nature, 1960. **187**: p. 493 - 494.
2. A. Javan, W.R.B.J., and D. R. Herrott, *Population inversijon and continuous optical maser oscillation in a gas discharge containing a He–Ne mixture.* Physical Review Letters 1961. **6**: p. 106–110.
3. Hall, R.N.G.E.F., J. D. Kingsley, T. J. Soltys, and R. O. Carlson *Coherent Light Emission From GaAs Junctions.* Physical Review Letters, 1962. **9**: p. 366–369.
4. P. P. Sorokin, J.R.L., *Stimulated Emission Observed from an Organic Dye, Chloro-aluminum Phthalocyanine.* IBM Journal of Research and Development, 1966. **10**(2): p. 162.
5. P. A. Franken, A.E.H., C. W. Peters, and G. Weinreich, *Generation of Optical Harmonics.* Physical Review Letters, 1961. **7**: p. 118.
6. J. A. Armstrong, N.B., J. Ducuing, and P. S. Pershan, *Interactions between Light Waves in a Nonlinear Dielectric.* Physical Review, 1962. **127**: p. 1918 - 1939.
7. G. Malka, J.F., F. Amiranoff, S. D. Baton, R. Gaillard, J. L. Miquel, H. Pépin, C. Rousseaux, G. Bonnaud, M. Busquet, and L. Lours, *Suprathermal Electron Generation and Channel Formation by an Ultrarelativistic Laser Pulse in an Underdense Preformed Plasma.* Physical Review Letters, 1997. **79**: p. 2053 - 2056.
8. A. Pukhov, Z.M.S., J. Meyer-ter-Vehn, *Particle acceleration in relativistic laser channels.* Physics of Plasmas, 1999. **6**: p. 2847
9. Gahn, C.T., G. D.; Pukhov, A.; Meyer-Ter-Vehn, J.; Pretzler, G.; Thirolf, P.; Habs, D.; Witte, K. J., *Multi-MeV Electron Beam Generation by Direct Laser Acceleration in High-Density Plasma Channels.* Physical Review Letters, 1999. **83**(23): p. 4772-4775.
10. Meyer-ter-Vehn, A.P.a.J., *Relativistic Magnetic Self-Channeling of Light in Near-Critical Plasma: Three-Dimensional Particle-in-Cell Simulation.* Physical Review Letters, 1996. **76**: p. 3975 - 3978.
11. G. Pretzler, A.S., A. Pukhov, D. Rudolph, T. Schätz, U. Schramm, P. Thirolf, D. Habs, K. Eidmann, G. D. Tsakiris, J. Meyer-ter-Vehn, and K. J. Witte, *Neutron production by 200 mJ ultrashort laser pulses.* Physical Review E 1998. **58**: p. 1165 - 1168.
12. L. Disdier, J.-P.G., G. Malka, and J-L. Miquel, *Fast Neutron Emission from a High-Energy Ion Beam Produced by a High-Intensity Subpicosecond Laser Pulse.* Physical Review Letters, 1999. **82**: p. 1454 - 1457.
13. J. Zweiback, R.A.S., T. E. Cowan, G. Hays, K. B. Wharton, V. P. Yanovsky, and T. Ditmire, *Nuclear Fusion Driven by Coulomb Explosions of Large Deuterium Clusters.* Physical Review Letters, 2000. **84**: p. 2634 - 2637.
14. Waynant, R.W.a.E., M.N, *ELECTRO-OPTICS HANDBOOK*. 2nd Ed ed, ed. M.N.E. Ronald W. Waynant. 2000, New York: McGraw- Hill.
15. Gerard A. Mourou, D.D., Subrata K. Dutta, Victor Elner, Ron Kurtz, Paul R. Lichter, Xinbing Liu, Peter P. Pronko, Jeffrey A. Squier, *Method for controlling configuration of laser induced breakdown and ablation*. 1997. p. 21.
16. P.P. Pronko, S.K.D., J. Squier, J.V. Rudd, D. Du, and G. Mourou, *Machining of sub-micron holes using a femtosecond laser at 800 nm* Optics Communications, 1995. **114**(1): p. 106-110.
17. F. Korte, S.A., A. Egbert, C. Fallnich, A. Ostendorf, S. Nolte, M. Will, J.-P. Ruske, B. N. Chichkov, A. T¨unnermann, *Sub-diffraction limited structuring of solid targets with femtosecond laser pulses.* Optics Express, 2000. **7**(2): p. 41-49.
18. A.P. Joglekar, H.L., G.J. Spooner, E. Meyhöfer, G. Mourou and A.J. Hunt, *A study of the deterministic character of optical damage by femtosecond laser pulses and applications to nanomachining* Applied Physics B: Lasers and Optics, 2003. **77**(1): p. 25-30.
19. Linjie Li, J.T.F., *Multiphoton polymerization.* Materials Today, 2004. **10**(6): p. 30-37.
20. Leong, K.H.S., A.A. Maynard, R. *Femtosecond micromachining applications for electro-optic components*. in *Electronic Components and Technology Conference*. 2001. Orlando, FL
21. N. Sanner, N.H., E. Audouard, C. Larat, P. Laporte, J. P. Huignard, *100-kHz diffraction-limited femtosecond laser micromachining.* Applied Physics B, 2005. **80**(1): p. 27-30.
22. Niemz, Y.L.a.M., *Ablation of femural bone with femtosecond laser pulses—a feasibility study.* Lasers in Medical Science, 2007. **22**(3): p. 171-174.

23. G. Kamlage, T.B., A. Ostendorf and B.N. Chichkov, *Deep drilling of metals by femtosecond laser pulses* Applied Physics A, 2003. **77**(2): p. 307-310.
24. Niemz MH, K.A., Strassl M, Bäcker A, Beyertt A, Nickel D, Giesen A., *Tooth ablation using a CPA-free thin disk femtosecond laser system.* Applied physics. B, 2004. **79**(3): p. 269-271.
25. Fan, T.Y., *Heat generation in Nd:YAG and Yb:YAG.* Quantum Electronics, 1993. **29**(6): p. 1457 - 1459.
26. Krupke, W.F., *Ytterbium solid-state lasers. The first decade.* Quantum Electronics 2000. **6**(6): p. 1287-1296.
27. Miller A., F.D.M., *Laser Sources and Applications*. A NATO Advanced Study Institute, ed. M. A. 1997, Philadelphia, PA, U.S.A.: Institute of Physics Publishing.
28. A.Krueger, P.F., P.Herrmann, *Ytterbium-Tungstate Crystal Boosts High-Power Ultrafast Lasers.* Europhotonics, 2004: p. 24.
29. D. M. Rines, P.F.M., D. Welford, and G. A. Rines, *High-energy operation of a Co:MgF2 laser.* Optics Letters, 1994. **19**(9): p. 628-630.
30. Koechner, W., *Solid-State Laser Engineering*. 6th, rev ed. 2006: Springer.
31. Kutovoi, S.A.A., A.Y.; Khait, V.L.; Kuzmin, O.V.; Mikhailov, V.A.; Hinz, A.; Pfeifer, E. *Flash lamp pumped Cr,Nd:LSB laser with 6,30% efficiency*. in *Lasers and Electro-Optics Europe*. 1994.
32. Weber, M.J., *Handbook of Lasers*. 2001, Boca Raton: CRC.
33. D. Parsons-Karavassilis, R.J., M. J. Cole, P. M. W. French, J. R. Taylor, *Diode-pumped all-solid-state ultrafast Cr :LiSGAF laser oscillator-amplifier system applied to laser ablation.* Optics communications, 2000. **175**(4-6): p. 389-396.
34. Torizuka, S.U.a.K., *Generation of 12-fs pulses from a diode-pumped Kerr-lens mode-locked Cr:LiSAF laser.* Opt. Lett, 1999. **24**: p. 780-782.
35. P. Wagenblast, U.M., F. Grawert, F. X. Kärtner. *12-fs, diode-pumped Cr3+:LiCAF laser.* in *CLEO*. 2003.
36. Aoshima, S.I., H.; Tsuchiya, Y, *Compact geometry for diode-pumped Cr:LiSAF femtosecond laser.* Quantum Electronics, 1997. **3**(1): p. 95 - 99.
37. A. Isemann, P.W.e., C. Fallnich, *Directly diode-pumped Colquiriite regenerative amplifiers.* Optics Communications, 2006. **260**(1): p. 211-222
38. A. Agnesi, C.P., G. C. Reali, and V. Kubecek *High-power diode-pumped picosecond Nd3+:YVO4 laser.* Optics Letters, 1997. **22**(21): p. 1645-1647.
39. D. Kopf, F.X.K., U. Keller, and K. J. Weingarten, *Diode-pumped mode-locked Nd:glass lasers with an antiresonant Fabry-Perot saturable absorber.* Opt. Lett, 1995. **20**: p. 1169-
40. Wei Lua, L.Y.a.C.R.M., *Kerr-lens mode-locking of Nd:glass laser* Optics Communications, 2001. **200**(1-6): p. 159-163
41. F. Brunner, T.S., E. Innerhofer, F. Morier-Genoud, R. Paschotta, V. E. Kisel, V. G. Shcherbitsky, N. V. Kuleshov, J. Gao, K. Contag, A. Giesen, and U. Keller, *240-fs pulses with 22-W average power from a mode-locked thin-disk Yb:KY(WO4)2 laser.* Opt. Lett, 2002. **27**: p. 1162-1164.
42. Liu, H.-h.N., John; Mourou, Gerard, *Directly diode-pumped Yb:KY(WO4)2 regenerative amplifiers.* Optics Letters, 2002. **27**(9): p. 722-724.
43. Liu, H.N., J.; Mourou, G.; Biswal, S.; Spühler, G. J.; Keller, U.; Kuleshov, N. V., *Yb:KGd(WO4)2 chirped-pulse regenerative amplifiers.* Optics Communications, 2002. **203**(3-6): p. 315-321.
44. Antoine Courjaud, R.M.-R., Nelly Deguil, Clemens Hönninger and François Salin. *Diode-pumped Multikilohertz Yb:KGW Femtosecond Amplifier*. in *CLEO*. 2002.
45. F. Druon, S.C., P. Raybaut, F. Balembois, P. Georges, R. Gaumé, G. Aka, B. Viana, D. Vivien, J.P. Chambaret, S. Mohr, D. Kopf, *Largely tunable diode-pumped sub-100-fs Yb:BOYS laser.* Applied Physics B-Lasers and Optics, 2002. **74**: p. s201-s203.
46. F. Brunner, G.J.S., J. A. d. Au, L. Krainer, F. Morier-Genoud, R. Paschotta, N. Lichtenstein, S. Weiss, C. Harder, A. A. Lagatsky, A. Abdolvand, N. V. Kuleshov, and U. Keller, *Diode-pumped femtosecond Yb:KGd(WO4)2 laser with 1,1-W average power.* Opt. Lett, 2000. **25**: p. 1119-1121.
47. P. Klopp , V.P., and U. Griebner, G. Erbert, *Passively mode-locked Yb:KYW laser pumped by a tapered diode laser.* OPTICS EXPRESS, 2002. **10**(2): p. 108-113.
48. H. Liu, J.N., and G. Mourou *Diode-pumped Kerr-lens mode-locked Yb:KY(WO4)2 laser.* Optics Letters, 2001. **26**(21): p. 1723-1725.

49. Daniel J. Ripin, J.R.O., R. L. Aggarwal, and Tso Yee Fan, *165-W cryogenically cooled Yb:YAG laser.* Optics Letters, 2004. **29**(18): p. 2154-2156.
50. Shen, Y.R., *The Principles of Nonlinear Optics*. 1984, New York: Wiley-Interscience.
51. Rullière, C., *Femtosecond Laser Pulses: Principles and Experiments*. Second Edition ed, ed. C. Rulli`ere. 2003: Springer.
52. LeBlanc, C., P. Curley, and F. Salin, *Gain-narrowing and gain-shifting of ultra-short pulses in Ti:sapphire amplifiers.* Optics Communications, 1996. **131**(4-6): p. 391-398.
53. Romero, J.J., et al., *Continuous-wave laser action of Yb3+-doped lanthanum scandium borate.* Applied Physics B-Lasers and Optics, 2005. **80**(2): p. 159-163.
54. Rivier, S., et al., *Ultrashort pulse Yb : LaSc3(BO3)(4) mode-locked oscillator.* Optics Express, 2007. **15**(23): p. 15539-15544.
55. Petermann, K., et al., *Highly Yb-doped oxides for thin-disc lasers.* Journal of Crystal Growth, 2005. **275**(1-2): p. 135-140.
56. Jiang, H.D., et al., *Spectral and luminescent properties of Yb3+ ions in YCa4O(BO3)(3) crystal.* Chemical Physics Letters, 2002. **361**(5-6): p. 499-503.
57. Chenais, S., et al., *Multiwatt, tunable, diode-pumped CWYb : GdCOB laser.* Applied Physics B-Lasers and Optics, 2001. **72**(4): p. 389-393.
58. Taira, T., *RE3+-ion-doped YAG ceramic lasers.* Ieee Journal of Selected Topics in Quantum Electronics, 2007. **13**(3): p. 798-809.
59. Lagatsky, A.A., N.V. Kuleshov, and V.P. Mikhailov, *Diode-pumped CW lasing of Yb : KYW and Yb : KGW.* Optics Communications, 1999. **165**(1-3): p. 71-75.
60. Druon, F., et al., *Largely tunable diode-pumped sub-100-fs Yb : BOYS laser.* Applied Physics B-Lasers and Optics, 2002. **74**: p. S201-S203.
61. Klopp, P., et al., *Highly efficient mode-locked Yb : Sc2O3 laser.* Optics Letters, 2004. **29**(4): p. 391-393.
62. Rico, M., et al., *Tunable laser operation of ytterbium in disordered single crystals of Yb : NaGd(WO4)(2).* Optics Express, 2004. **12**(22): p. 5362-5367.
63. Petrov, V., et al., *Continuous-wave laser operation of disordered double tungstate and molybdate crystals doped with ytterbium.* Journal of Non-Crystalline Solids, 2006. **352**(23-25): p. 2371-2375.
64. Druon, F., et al., *Generation of 90-fs pulses from a mode-locked diode-pumped Yb3+: Ca4GdO(BO3)(3) laser.* Optics Letters, 2000. **25**(6): p. 423-425.
65. Gaume, R., et al., *Mechanical, thermal and laser properties of Yb : (Sr1-xCax)(3)Y(BO3)(3) (Yb : CaBOYS) for 1 mu m laser applications.* Optical Materials, 2003. **24**(1-2): p. 385-392.
66. Saikawa, J., et al., *Femtosecond Yb3+-doped Y-3(Sc0.5Al0.5)(2)O-12 ceramic laser.* Optical Materials, 2007. **29**(10): p. 1283-1288.
67. Snitzer, E., *Proposed fiber cavities for optical masers.* J. Appl. Phys, 1961. **23**(1): p. 36.
68. A. Giesen, H.H., A. Voss, K. Wittig, U. Brauch, H. Opower, *Scalable concept for diode-pumped high-power solid-state lasers.* Applied Physics B, 1994. **58**(5): p. 365-372.
69. Limpert, J., et al., *Extended single-mode photonic crystal fiber lasers.* Optics Express, 2006. **14**(7): p. 2715-2720.
70. Shoji, T., et al., *Quantum-defect-limited operation of diode-pumped Yb : YAG laser at low temperature.* Japanese Journal of Applied Physics Part 2-Letters & Express Letters, 2004. **43**(4A): p. L496-L498.
71. F. Hoos, S.L., T. P. Meyrath, B. Braun and H. Giessen, *Thermal lensing in an end-pumped Yb:KGW slab laser with high power single emitter diodes.* Optics Express, 2008. **16**(9): p. 6041-6049.
72. Vittorio Magni, G.C.a.S.D.S., *ABCD matrix analysis of propagation of gaussian beams through Kerr media.* Optics Communications, 1993. **96**: p. 348-355.
73. Keller, U.W., K.J.; Kartner, F.X.; Kopf, D.; Braun, B.; Jung, I.D.; Fluck, R.; Honninger, C.; Matuschek, N.; Aus der Au, J., *Semiconductor saturable absorber mirrors (SESAMapos;s) for femtosecondto nanosecond pulse generation in solid-state lasers.* Quantum Electronics, 1996. **2**(3): p. 435 - 453.
74. Vittorio Magni, G.C.a.S.D.S., *Closed form Gaussian beam analysis of resonators containing a Kerr medium for femtosecond lasers.* Optics Communications, 1993. **101**(5-6): p. 365-370.

75. C. Hönninger, R.P., F. Morier-Genoud, M. Moser, and U. Keller *Q-switching stability limits of continuous-wave passive mode locking.* J. Opt. Soc. Am. B, 1999. **16**(1): p. 46-56.
76. Spence, D.E., P.N. Kean, and W. Sibbett, *60-Fsec Pulse Generation from a Self-Mode-Locked Ti-Sapphire Laser.* Optics Letters, 1991. **16**(1): p. 42-44.
77. Salin, F., J. Squier, and M. Piche, *Mode-Locking of Ti-Al2o3 Lasers and Self-Focusing - a Gaussian Approximation.* Optics Letters, 1991. **16**(21): p. 1674-1676.
78. Chen, S.Y. and J.Y. Wang, *Self-Starting Issues of Passive Self-Focusing Mode-Locking.* Optics Letters, 1991. **16**(21): p. 1689-1691.
79. Uemura, S. and K. Torizuka, *Generation of 12-fs pulses from a diode-pumped Kerr-lens mode-locked Cr : LiSAF laser.* Optics Letters, 1999. **24**(11): p. 780-782.
80. Russbuldt, P., D. Hoffmann, and R. Poprawe, *Generation of 13.5-fs pulses from a diode-pumped Kerr-lens modelocked Drismless Cr : LiSGaF laser - art. no. 61000K.* Solid State Lasers XV: Technology and Devices, 2006. **6100**: p. K1000-K1000

553.

81. Lagatsky, A.A., et al., *Yb3+-doped YVO4 crystal for efficient Kerr-lens mode locking in solid-state lasers.* Optics Letters, 2005. **30**(23): p. 3234-3236.
82. Jean-Claude Diels, W.R., Paul Liao and Paul Kelley, *Ultrashort Laser Pulse Phenomena : Fundamentals, Techniques and Applications on a Femtosecond Time Scale.* 1996: Academic Press.
83. F. X. Kärtner, I.D.J.i.U.K., *Soliton Mode-Locking with Saturable Absorbers.* Quantum Electronics, 1996. **2**(3): p. 540 - 556.
84. Molis, G.A., R.; Krotkus, A.; Bertulis, K.; Giniunas, L.; Pocius, J.; Danielius, R., *Terahertz time-domain spectroscopy system based on femtosecond Yb:KGW laser.* Electronics Letters, 2007. **43**(3): p. 190 - 191.
85. Perry, M., *Multilayer dielectric gratings.* Science and Technology review, 1995(September): p. 24-33.
86. Z.L.Horvath, K.O., Z.Bor, *Dispersed femtosecond pulses in the vicinity of focus.* Optics Communications, 1994. **111**(5-6): p. 478-482.
87. J.Faure, J.I., S.Biswal, G.Cheriaux, L.Bruner, G.C.Templeton, and G.Mourou, *A spatially dispersive regenerative amplifier for ultrabroadband pulses.* Optics Communications, 1999. **159**(1-3): p. 68-73.
88. Christov, I.P., *Amplification of femtosecond pulses in a spatially dispersive scheme.* Optics Letters, 1992. **17**(10): p. 742-744
89. C. P. Hauri, M.B., W. Kornelis, J. Biegert, and U. Keller *Generation of 14.8-fs pulses in a spatially dispersed amplifier.* Optics Letters, 2004. **29**(2): p. 201-203
90. C.LeBlanc, G.G., J.P.Chambaret, A.Migus, and A.Antonetti, *Compact and efficient multipass Ti:sapphire system for femtosecond chirped-pulse amplification at the terawatt level.* Optics Letters, 1993. **18**(2): p. 140-142
91. R. Trebino, K.W.D., D.N. Fittinghoff, J.N. Sweetser, M.A. Krumbugel, B.A. Richman, D.J. Kane, *Measuring ultrashort laser pulses in the time-frequency domain using frequency-resolved optical gating.* Review of Scientific Instruments, 1997. **68**(9): p. 3277.
92. Linden, S.G., H. Kuhl, J., *XFROG: new method for amplitude and phase characterization ofultraweak ultrashort pulses.* Phys. Stat. Sol. (b), 1998. **206**(1): p. 119-124.
93. Sandor Szatmari, P.S., and Matthias Feuerhake, *Group-velocity-dispersion-compensated propagation of short pulses in dispersive media.* Optics Letters, 1996. **21**(15): p. 1156-.
94. Z. Sacks, G.M., and R. Danielius *Adjusting pulse-front tilt and pulse duration by use of a single-shot autocorrelator.* Optics Letters, 2001. **26**(7): p. 462-464.